NASA Contractor
Report No. 66519A

Research and Development Program for a Combined Carbon Dioxide Removal and Reduction System - Supplement 1

J.O'M. BOCKRIS
A. CALANDRA
C. SOLOMONS
(UNIVERSITY OF PENNSYLVANIA)

Contract No. NAS 1-4154
Final Report - Phase II A
HSER 4908 Supplement 1
February,1969

Hamilton Standard DIVISION OF UNITED AIRCRAFT CORPORATION UA®

RESEARCH and DEVELOPMENT PROGRAM for a COMBINED CARBON DIOXIDE REMOVAL AND REDUCTION SYSTEM

PHYSICOCHEMICAL PROPERTIES OF LITHIUM CHLORIDE LITHIUM CARBONATE MELT MIXTURES

Contract NAS 1-4154
Final Report - Phase IIA.
HSER 4908 Supplement 1

February, 1969

PHYSICOCHEMICAL PROPERTIES OF LITHIUM CHLORIDE-LITHIUM CARBONATE MELT MIXTURES

ABSTRACT

Experimental studies of liquid mixtures of lithium chloride and lithium carbonate were conducted at temperatures between 550° C and 800°C for a range of compositions including the eutectic. Viscosity, density, and surface tension were measured by suitable modifications of a linear oscillation viscometer. Contact angles with POCO AX and spectroscopically pure graphite were also observed as functions of composition and temperature. Self-diffusion coefficients for carbonate ions in the eutectic mixture were determined by radioisotope tagging of carbonate ions with C^{14}, enabling measurement of diffusion of carbonate into a capillary tube from an external phase. Laboratory techniques, evaluation of precision, and measured physico-chemical properties are presented in detail.

FOREWORD

This supplement has been prepared by the Electrochemistry Laboratory of the John Harrison Laboratory of Chemistry, University of Pennsylvania, Philadelphia, Pennsylvania,and is part of the effort required by National Aeronautics and Space Administration Contract No. NAS 1-4154, Phase IIA, entitled "Research and Development Program for a Combined Carbon Dioxide Removal and Reduction System." The work here reported was performed under a subcontract between Hamilton Standard, Division of United Aircraft Corporation, and the University of Pennsylvania, whereby the Electrochemistry Laboratory was authorized to study and measure certain physicochemical properties of fused lithium chloride-lithium carbonate mixtures under consideration as electrolytes in the carbon dioxide removal and reduction system.

The studies were performed by Dr. Cyril Solomons and Dr. Alfredo Calandra under the direction of Professor John O'M. Bockris, during the period, September, 1967, through January, 1969.

LIST OF FIGURES

LIST OF FIGURES (Continued)

LIST OF TABLES

LIST OF TABLES (CON'T)

PHYSICOCHEMICAL PROPERTIES OF

LITHIUM CHLORIDE-LITHIUM CARBONATE MELT MIXTURES

Part I

VISCOSITY, DENSITY AND SURFACE TENSION OF MOLTEN LITHIUM CHLORIDE-LITHIUM CARBONATE MIXTURES

GENERAL

The eutectic mixture of lithium chloride and lithium carbonate (70:30 mole %) is of potential use as the electrolyte in a cell for the regeneration of oxygen from carbon dioxide. Such a cell is under study by NASA for use in manned spacecraft life-support systems. Little is known about the physicochemical properties of this system, however. The present Section describes studies which have been made of the surface tensions, contact angles against various materials, densities and viscosities of various mixtures of lithium chloride with lithium carbonate in an endeavor to fill this gap and provide a basis for a structural understanding of these systems. Some additional measurements of the effect of added Li_2O are also reported.

EXPERIMENTAL

Introduction

The linear-oscillation viscometer [1-4] serves both as a viscometer, when a thin plate is used, and as an Archimedean densitometer, when a solid body is used. By a slight modification of the cell, in which the spiral spring-based viscometer is mounted, it has become possible to extend the usefulness of this device even further. With this modification, absolute measurements of surface tension by the "pull-plate" method can readily and accurately be made. A single device can thus be used for three common physicochemical studies merely by changing the form of the suspended object as appropriate.

The Cell and Mechanical Apparatus

In Figure 1 is shown a schematic diagram of the oscillating plate viscometer, which has already been described in detail elsewhere [1,3]. When the plate P is replaced by a solid object (e.g., a ball or cylinder) of known volume (V_S), the loss in weight (ΔW_g) of the object on immersion in a liquid provides a measure of the density (ρ_L) of the liquid according to:

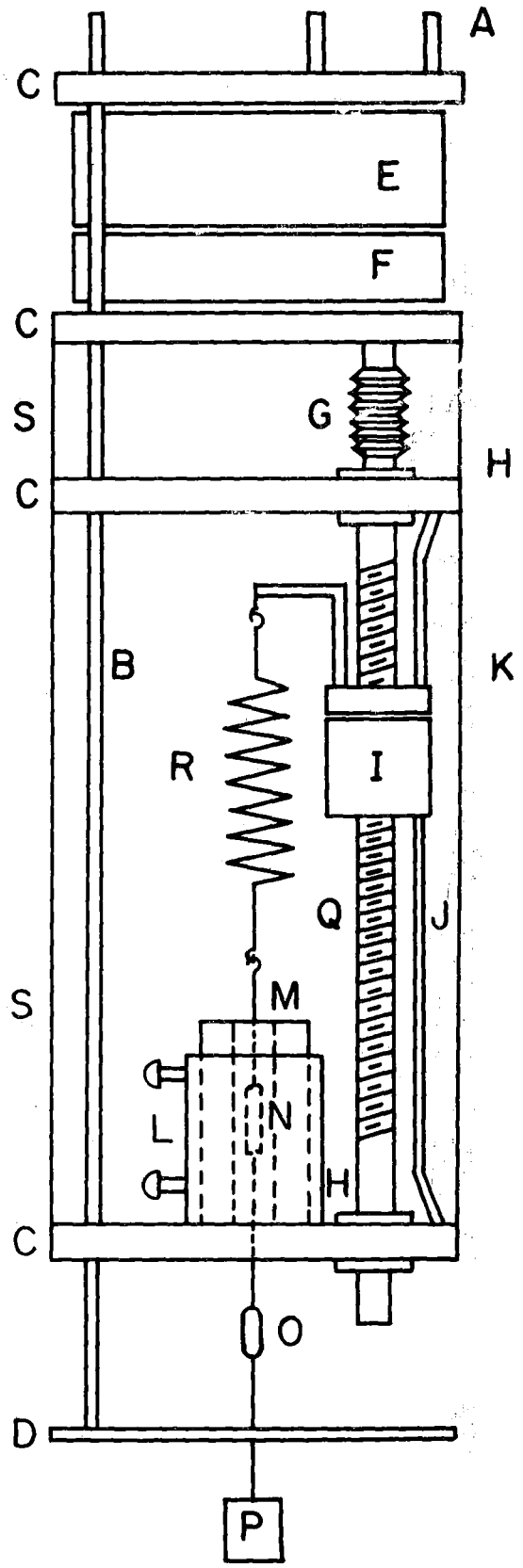

Figure 1. Oscillating Plate Viscometer

$$\Delta W_g = V_s \rho_L$$

where ρ_L is expressed in g ml^{-1}.

In this apparatus, the mechanical motion system provided by the motor E, gear train F, coupling G, threaded rod Q, and drive block I, serve to permit centralizing adjustments of the LVDT* transducer core N in the housing M. This mechanism allows for compensation of the motion of the core due to pressure or temperature changes of the liquid, when the viscosity is to be measured.

When the density is required, the difference of the LVDT readings with and without the liquid surrounding the solid body is readily obtained at room pressure, especially if the apparatus is not sealed to provide a controlled atmosphere.

For use as an apparatus to measure surface tension, however, measurements are needed under a given set of conditions with the plate not touching and just touching the surface. To achieve the latter conditions, it is necessary to separate, slowly and continuously, the liquid and the plate. Therefore, the method used for the density measurements could not be used with the surface tension apparatus. It would be possible, in theory, to use the motorized drive system described above to achieve the desired separation; but in such a case it is difficult to isolate the change in LVDT reading produced by the change in surface tension pull from the change in reading produced by a shift in core position due to movement of the upper end of the spring. Furthermore, practical trials showed that a considerable amount of vibration was imparted to the LVDT core, which resulted in noise in the output signal from the LVDT, when the spring was moved directly.

A satisfactory solution was accomplished by providing a mechanism for altering the position of the container for the liquid, relative to the plate. In the apparatus actually constructed, a controlled environment was desired, but measurements were to be made at 1 atm pressure; hence, the specially-designed but very simple device shown in Figure 2 was constructed.

The mechanical drives A and B at top and bottom of the cell were constructed from Delmar-Umy Type DM850 teflon high-vacuum stopcocks. These stopcocks are satisfactory for use down to 10^{-6} Torr; hence, the atmosphere within the cell can readily be controlled or changed. In their original state they permit nearly 2.0 cm of linear motion to be achieved smoothly and slowly by manual rotation of the external finger-grip; by the modification this can be increased to 3.7 cm. The top drive is used to centralize the core of the LVDT; the bottom one serves to raise and lower the container of liquid.

*Linear Variable Differential Transformer.

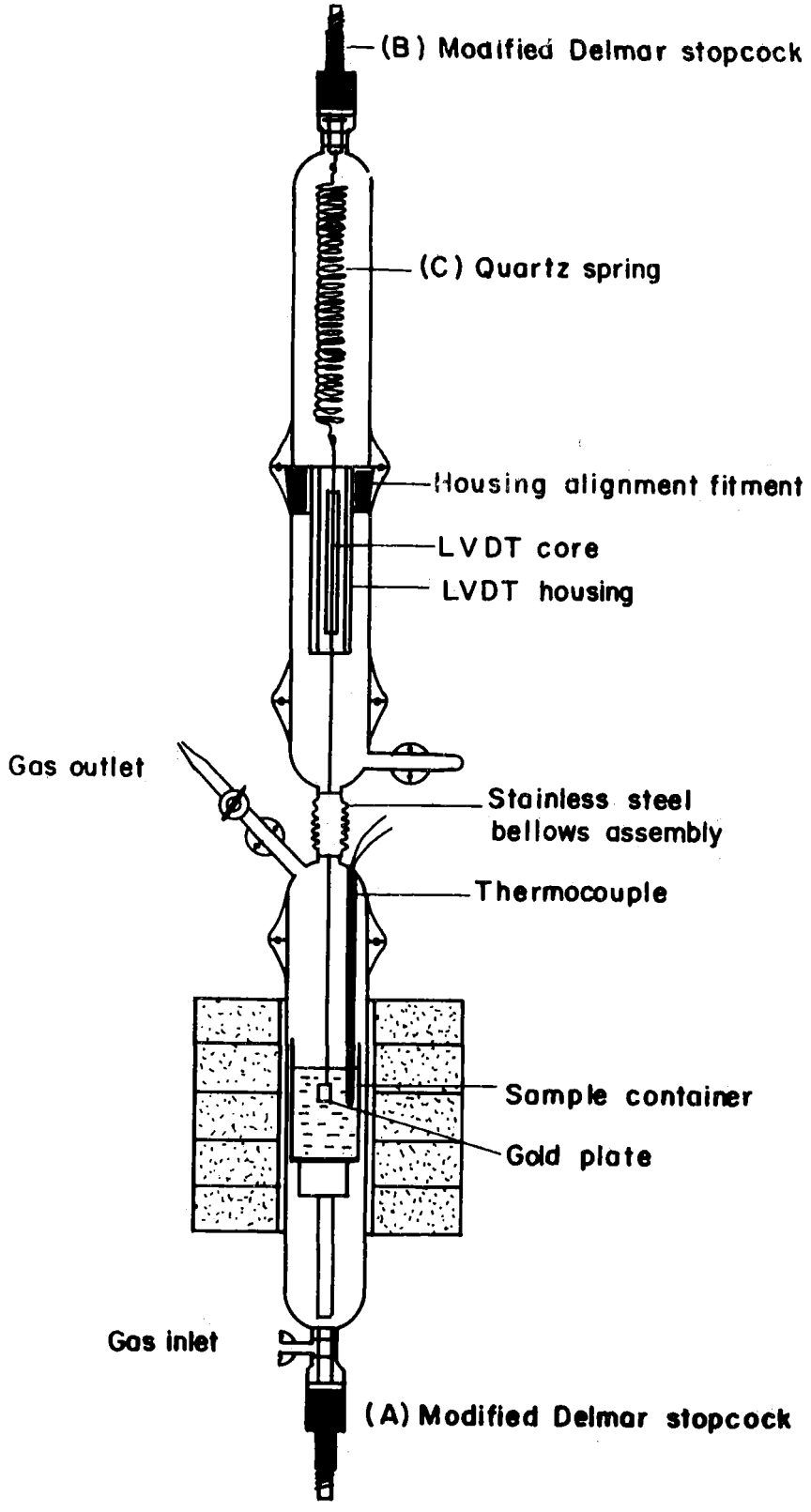

Figure 2. Diagram of the Modified Oscillating Plate Viscometer

For many purposes a much simpler cell than the one shown could be used. In our studies it was desired to reduce to a minimum any sample vaporization or hot air convection into the upper parts of the cell, and to provide means for rapid disassembly and cleaning. Otherwise a simple tube-and-cap single-chamber type of cell could have been used. Furthermore, the long cell made alignment of the suspension system difficult without danger to the thin connecting tubes; therefore, it was found desirable to incorporate a flexible connection in our version, which could be omitted in a single-chamber cell.

Electrical System

Several changes were made to the electrical measuring system; some to upgrade the earlier apparatus [1,3], others to provide for greater convenience, particularly with the surface tension measurements.

The original LVDT was replaced by a Schaewitz 1000-XS-A-P, having a specially provided small diameter core. The linear range of this is some ±2 cm. Similarly, the original twin half-wave demodulator was replaced by the twin full-wave demodulator whose circuit is given in Figure 3. With this, a smoother output is obtained. The demodulator was constructed using 1N482B low-temperature coefficient diodes in the rectifier networks to provide greater temperature stability.

The fast-response recorder used in the original system was retained in the new version for viscosity measurements. For the density and surface tension measurements, however, there is no need to follow rapid changes of output signal from the demodulator, and a strip-chart recorder with a 25 cm wide chart was found to provide greater convenience and accuracy of reading.

Instead of the recorder, for density and surface tension measurements, and also for other "static" measurements such as calibration of the output signal versus spring motion relationship, a 5-dial digital millivoltmeter was often used; this was the fastest and most convenient method, but, of course, provided no permanent record from which accidental changes in the apparatus, drifts, etc., could be identified.

Operation of the Apparatus

The basic method of operation of the apparatus for viscosity and density studies can be seen from the design of the apparatus (Fig. 2) and from the description given previously [1,3]. Thanks to the mechanical drive at the bottom of the cell, the taking of readings "in gas" and "in liquid" within a few moments of each other can be performed with ease. Thus, the logarithmic damping of the plate in the gas and in the liquid, or the upthrusts on the solid body in the same media, can be measured within a

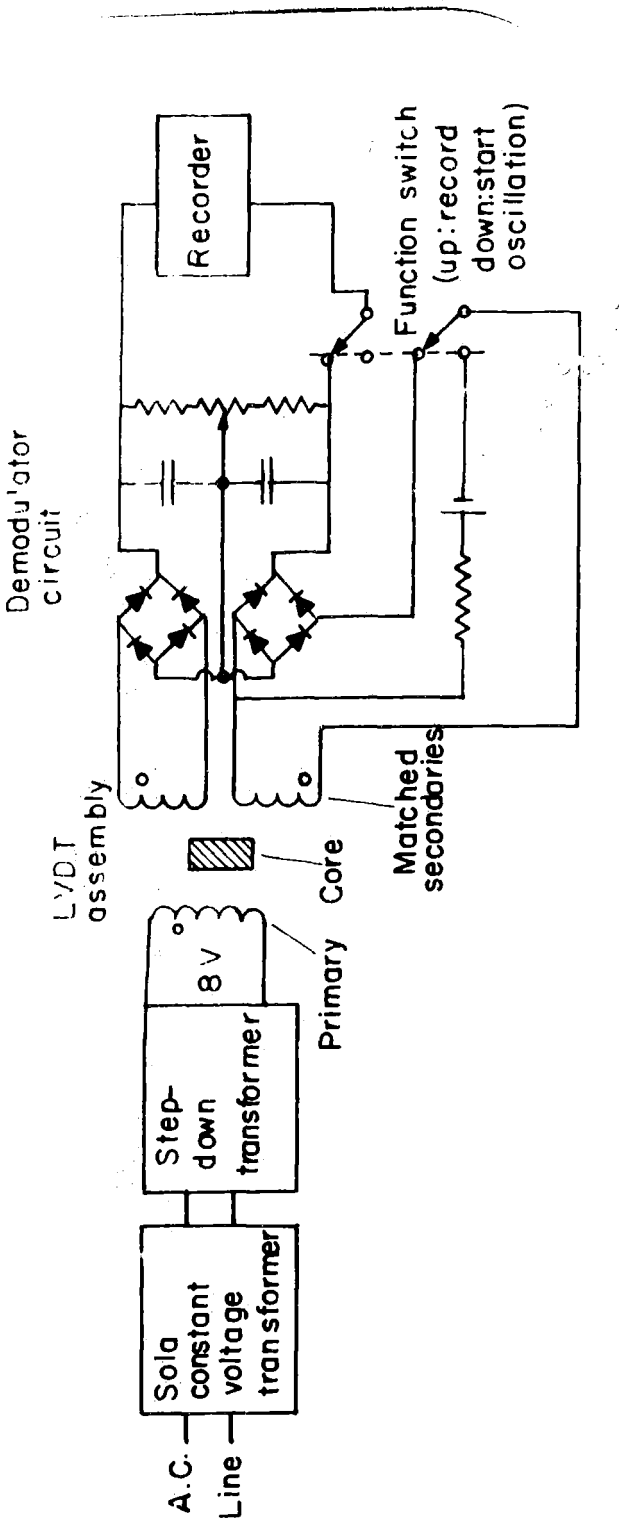

Figure 3. LVDT Operating Circuit

short enough period of time for all other experimental conditions to be sensibly constant.

In the case of surface tension studies, the liquid is brought up to a level at which it wets several mm of the bottom of the plate, and then the liquid level is lowered slowly until the plate just pulls away from the surface. Just before the break, the plate is restrained by a downwards force due to the surface forces in the liquid, in addition to all other forces operating; after the break this force no longer participates. Thus, the difference measured before and after the break gives, directly, the pull on the plate due to the surface forces. When the plate is wet completely by the liquid, this pull is $L\gamma$ dyne, where L is the perimeter of the plate and γ is the surface tension of the liquid; if there is only partial wetting (contact angle θ greater than 0°), the pull is $L\gamma \cos \theta$. Whenever possible, therefore, the material of the plate should be chosen to provide $\theta = 0$.

In practice, as shown in Figure 4, the recording of spring load versus time (which roughly corresponds, if the operation is performed reasonably smoothly, to liquid level) does not exhibit a perfect square-topped trace. Before the break, there are small changes in the buoyancy of the plate as it is withdrawn from the liquid, there are slight changes in the shape of the meniscus as it "necks off" when the break is imminent, and so on. After the break, the plate retains some liquid which adds to its effective weight. It has been found that very reproducible and accurate results can be obtained if the maximum load on the spring before the break, and the load on the spring with the plate dry, are used to compute the load difference corresponding to $L\gamma$.

Calibrations

For viscosity measurements it is necessary to know the equation that relates [3] the viscosity of the medium in which the plate is oscillating and the logarithmic decrement (δ). The apparatus was calibrated with five organic liquids at room temperature, and with molten potassium nitrate at four temperatures between 347°C and 471°C. The densities and viscosities of the organic liquids and molten salt used as calibrating materials were taken from the literature; they are presented in Table 1.

Figure 5 shows the excellent linear response curve of the viscometer, obtained by least squares reduction of the experimental data. The equation

$$\sqrt{\eta\rho} = 39.24\delta - 4.78\times10^{-2}$$

fits these data, where η and ρ are the viscosity and density of liquids, and δ is the logarithmic decrement given by

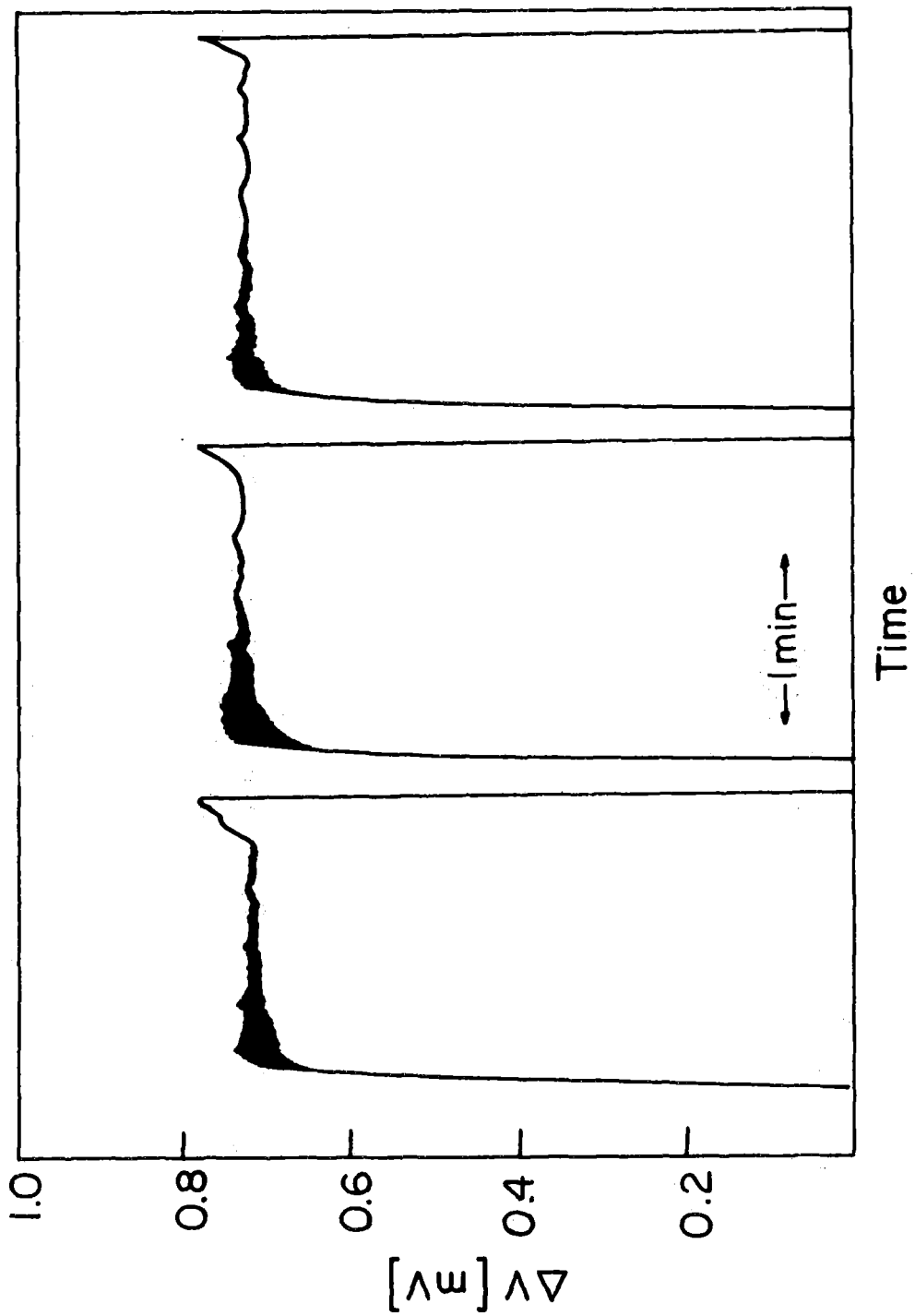

Figure 4. Recordings of Spring Load Versus Time Surface Tension Measurement (LiCl 80 Mole % - Li_2CO_3 20 Mole %; 553°C)

TABLE 1. VISCOSITY CALIBRATION DATA*

Calibration Substance	Logarithmic Decrement, δ	Density, ρ (g/cm^3)	Viscosity, η (cp)	$\sqrt{\eta\rho}$	Area Correction $(1+2\alpha\Delta t)$	Temp. (°C)
Carbon Tetrachloride	0.02967	1.5824	0.883	1.1830	-----	26.0
Chloroform	0.02225	1.4781	0.537	0.8913	-----	25.7
Benzene	0.01889	0.8728	0.592	0.7194	-----	26.0
Toluene	0.01804	0.8605	0.538	0.6808	-----	27.0
Nitrobenzene	0.03748	1.1965	1.723	1.435	-----	27.0
Potassium Nitrate	0.05873	1.8630	2.777	2.275	1.01056	347.0
Potassium Nitrate	0.05436	1.8389	2.343	2.075	1.01165	380.0
Potassium Nitrate	0.04868	1.8171	1.997	1.901	1.01264	410.0
Potassium Nitrate	o.04267	1.7726	1.539	1.652	1.01465	471.0

*References 5 and 6.

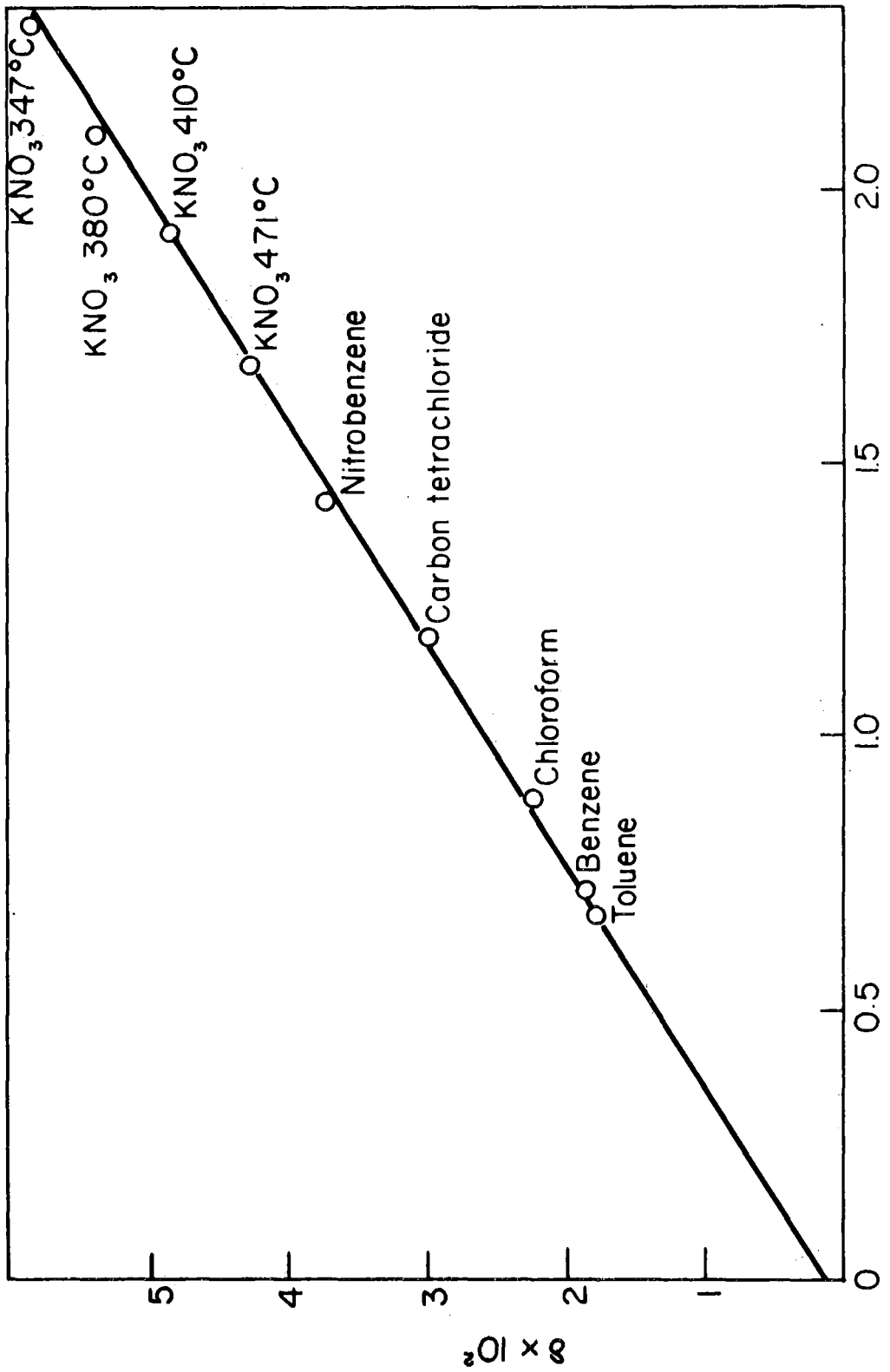

Figure 5. Logarithmic Decrement Versus $(\eta\rho)^{1/2}$ Calibration Plot

$$\delta = \frac{2.303}{n} \log \frac{A_0}{A_n}$$

where A_0 is the amplitude of an arbitrary "starting" oscillation and A_n is the amplitude of the n-th oscillation. In order to compensate for changes in the apparatus due to temperature, the equation [3,4]

$$\eta = \frac{1538.3}{(1+2\alpha\Delta t)^2 \rho} (\delta^2 - 2.43\times10^{-4}\delta)$$

must be used, where [7] α is the linear coefficient of the expansion of the material of the plate (gold), and Δt is the increment of temperature above 25°C. Besides, it is necessary to know that the LVDT demodulator output (in volts) is a linear function of spring extension. The density and surface tension measurements depend, however, on knowledge of the relationship of LVDT demodulator output to spring load (in grams).

To obtain all this information, a single set of measurements will suffice. The suspended plate or solid body is replaced by a small "balance pan" constructed from thin metal sheet (e.g., household aluminum foil) and support wires. A suitable index mark is located on some part of the system below the spring (a pointed fine wire tied temporarily to the bottom of the spring is excellent). Suitable weights are then placed in the "balance pan" while readings of spring extension are made optically with the aid of a cathetometer and readings of LVDT demodulator output are made using a 25 cm wide chart recorder (or, preferably, a digital millivoltmeter). With the springs we have used, for example, extensions of about 15 mm and LVDT outputs of 500 mV were obtained with a load of 3g; excellent linearity was observed over this range (e.g., 6.0134 mg mV^{-1} with a standard deviation of only 0.0066)

The volume of the solid body, used for density measurements by the Archimedean buoyancy method, must be known accurately. Owing to the shape of the body (e.g., the presence of a projecting ring for suspension) the preferred method of measuring its volume is to measure the buoyancies of the body in several liquids and calculate, using their densities, the volume displaced to give these buoyancies.

A check of the precision of the helical spring apparatus was made by comparing the volume of the bob (gold-palladium alloy) obtained using this apparatus with the volume of the same bob obtained by the use of the Mettler single-pan analytical balance. For this purpose benzene, toluene and carbon tetrachloride were used. The volume of the bob is given by:

$$V_0 = \frac{B + v + A}{\rho_C}$$

where ρ_c is the density of the reference liquid, B the buoyancy, v the correction to vacuo, and A is the surface tension effect on the suspension wire. The latter correction is given by:

$$A = \frac{\pi \gamma D}{g}$$

where D is the diameter of the suspension wire, γ is the surface tension of the reference liquid, and g is the gravitational constant. For measurements that are to be made at temperatures other than that at which the apparatus is calibrated, the change in volume of the immersed body can readily be taken into account using the thermal expansion coefficient for the gold-palladium alloy [8], (15.2×10^{-6}). The values of buoyancy and volume of the bob together with the densities [5] and surface tension [5] of the reference liquids are given in Table 2 for the Mettler balance, and in Table 3 for the helical spring apparatus.

The performance of this apparatus at high temperature was checked with molten potassium nitrate over the range 350°C to 450°C and molten sodium nitrate over the range 330°C to 460°C. In Figures 6 and 7, the values of densities obtained are compared with the literature data [8,9]. Tables 4 and 5 show the numerical values.

The surface tension measurement does not need a previous calibration because the perimeter of the plate (that is, the only parameter needed in the calculation) can be obtained by direct measurement of the edge length and thickness of the gold-palladium plate. This has been made with a pair of calipers with a precision of 0.05 mm. Nevertheless, it is convenient to check the system specially at high temperatures. For this purpose the surface tension of molten potassium and sodium nitrates were measured at temperatures covering the range of 320°C to 530°C for the former, and 350°C to 500°C for the latter. The values obtained are compiled in Tables 6 and 7, and in Figures 8 and 9. The results obtained for potassium nitrate are in good agreement with those reported in the literature [10,11]. The values for sodium nitrate are about 0.85 higher than those of the literature. The direction of the difference, and the parallelity of the plots, suggest that the material used in the reference cited may have contained some impurity (since contamination usually lowers the surface tension). For high temperature measurements the length correction for the perimeter of the plate due to expansion has been taken into account in the present work. The surface tension is given by:

$$\gamma = \frac{Wg}{2[L_{e_0} + L_{th_0})(1 + \alpha \Delta t)]}$$

where W is the maximum increase of the apparent weight of the plate, g is the gravitational constant, L_{e_0} and L_{th_0} are the length of the edge and the thickness, respectively, and α is the linear thermal expansion coefficient.

TABLE 2. DENSITY CALIBRATION DATA (METTLER)

Correction to vacuo v = 0.0013 g

Calibration Substance	Buoyancy, B (gram)	Surface Tension Correction, A (grams)	Density, ρ (g/cm^3) lit	Immersed Volume, V_0 (cm^3)	Temp. (°C)
Carbon Tetrachloride	1.7886	0.0012	0.5948	1.1231	19.5
Benzene	0.9849	0.0013	0.8794	1.1229	19.7
Toluene	0.9718	0.0013	0.8674	1.1234	19.5

V_0 average = 1.1231

NASA Contractor Report No. 66519A

TABLE 3. DENSITY CALIBRATION DATA (SPRING BALANCE)

			Correction to vacuo v = 0.0013 g			
Calibration Substance	Buoyancy, B (Volts)	Buoyancy, B (grams)	Surface Tension Correction, A (grams)	Density, ρ (g/cm^3) lit	Immersed Volume, V_0 (cm^3)	Temp. (°C)
Carbon Tetrachloride	0.29399	1.7679	0.00012	1.5786	1.1215	28.0
Benzene	0.16219	0.9753	0.00013	0.8717	1.1218	27.3
Toluene	0.16031	0.9641	0.00012	0.8604	1.1234	27.2

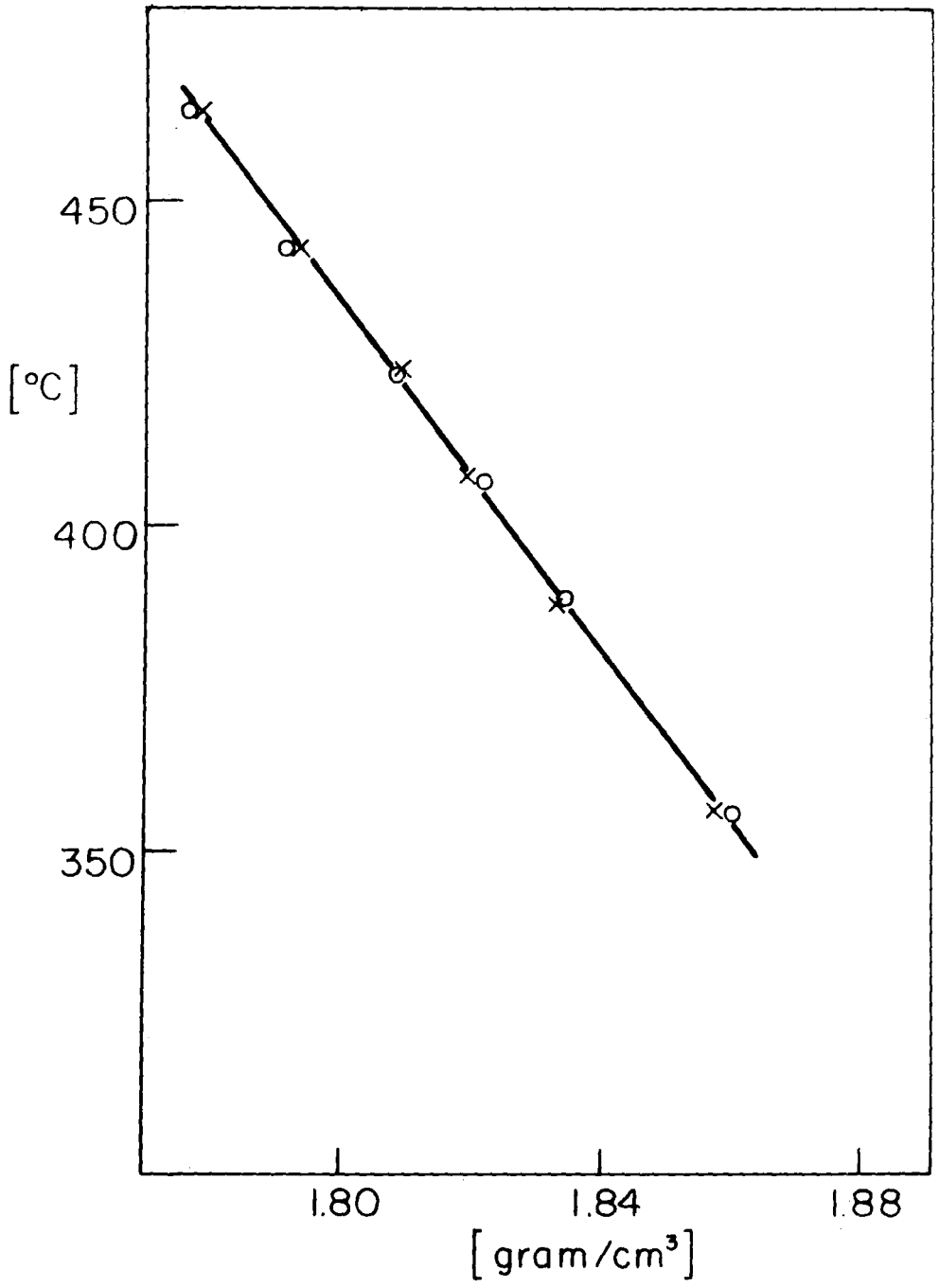

Figure 6. Density of Molten Potassium Nitrate. x: Janz and Lorenz; o: this work

TABLE 4. DENSITY OF MOLTEN POTASSIUM NITRATE

Correction to vacuo, v = 0.0005 g at 350°C

Temp. (°C)	Buoyancy B (Volts)	Buoyancy B (grams)	Surface Tension γ (dynes/cm)	Surface Tension Correction, A (grams)	Bob Volume V_T (cm^3)	Density (g/cm^3) Observed	lit[8]
356	0.35194	2.1164	108.2	0.0048	1.1408	1.8598	1.857
388	0.34753	2.0898	106.2	0.0047	1.1425	1.8337	1.833
407	0.34552	2.0778	104.9	0.0047	1.1435	1.8215	1.819
423	0.34326	2.0642	103.9	0.0046	1.1444	1.8081	1.808
443	0.34048	2.0475	102.6	0.0046	1.1455	1.7919	1.793
464	0.33795	2.0322	101.3	0.0045	1.1466	1.7767	1.778

TABLE 5. DENSITY OF MOLTEN SODIUM NITRATE

Correction to vacuo v = 0.0005 g at 350°C

Temp. (°C)	Buoyancy B (Volts)	Buoyancy B (grams)	Surface Tension γ (dynes/cm)	Surface Tension Correction, A (grams)	Bob Volume V_T (cm^3)	Density (g/cm^3) Observed	lit[9]
329	0.36036	2.1670	118.8	0.0053	1.1394	1.9069	1.903
348	0.35805	2.1531	117.5	0.0053	1.1404	1.8931	1.889
372	0.35535	2.1369	116.0	0.0052	1.1417	1.8767	1.873
392	0.35282	2.1217	114.7	0.0051	1.1428	1.8615	1.858
413	0.35054	2.1080	113.4	0.0051	1.1439	1.8477	1.844
435	0.34830	2.0945	112.0	0.0050	1.1451	1.8339	1.828
455	0.34608	2.0811	110.7	0.0050	1.1461	1.8206	1.814

TABLE 6. SURFACE TENSION OF MOLTEN POTASSIUM NITRATE

Temp. (°C)	Maximum Pull W (mV)	Maximum Pull W (grams)	Plate Perimeter (cm)	Surface Tension (dynes/cm)
354	21.50	0.12921	1.1290	112.3
368	21.45	0.12898	1.1292	112.1
368	21.35	0.12839	1.1292	111.5
384	21.00	0.12628	1.1295	109.7
405	20.67	0.12429	1.1299	107.9
428	20.10	0.12087	1.1303	104.9
464	19.65	0.11816	1.1309	102.5
494	18.98	0.11410	1.1315	98.9

TABLE 7. SURFACE TENSION OF MOLTEN SODIUM NITRATE

Temp. (°C)	Maximum Pull $\bar{W}$ (mV)	Maximum Pull W (grams)	Plate Perimeter (cm)	Surface Tension (dynes/cm)
345	22.85	0.13741	1.1288	119.4
373	22.45	0.13500	1.1293	117.3
411	21.98	0.13245	1.1300	114.7
445	21.40	0.12868	1.1306	111.7
475	21.18	0.12733	1.1311	110.4
505	20.90	0.12568	1.1317	108.9

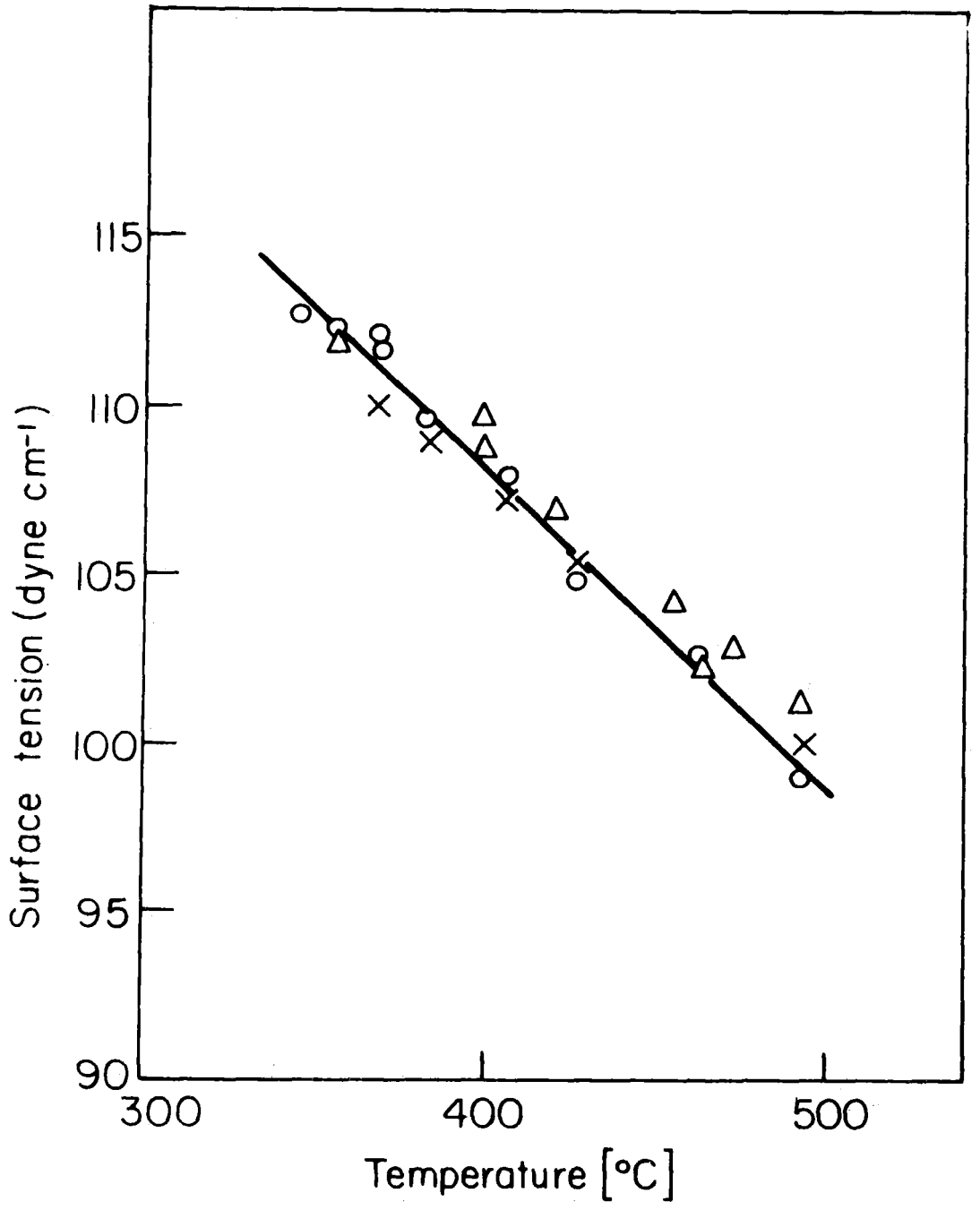

Figure 8. Surface Tension of Molten Potassium Nitrate. Δ: Dahl and Duke[11]; x: Bertozzi and Sternheim[10]; o: this work

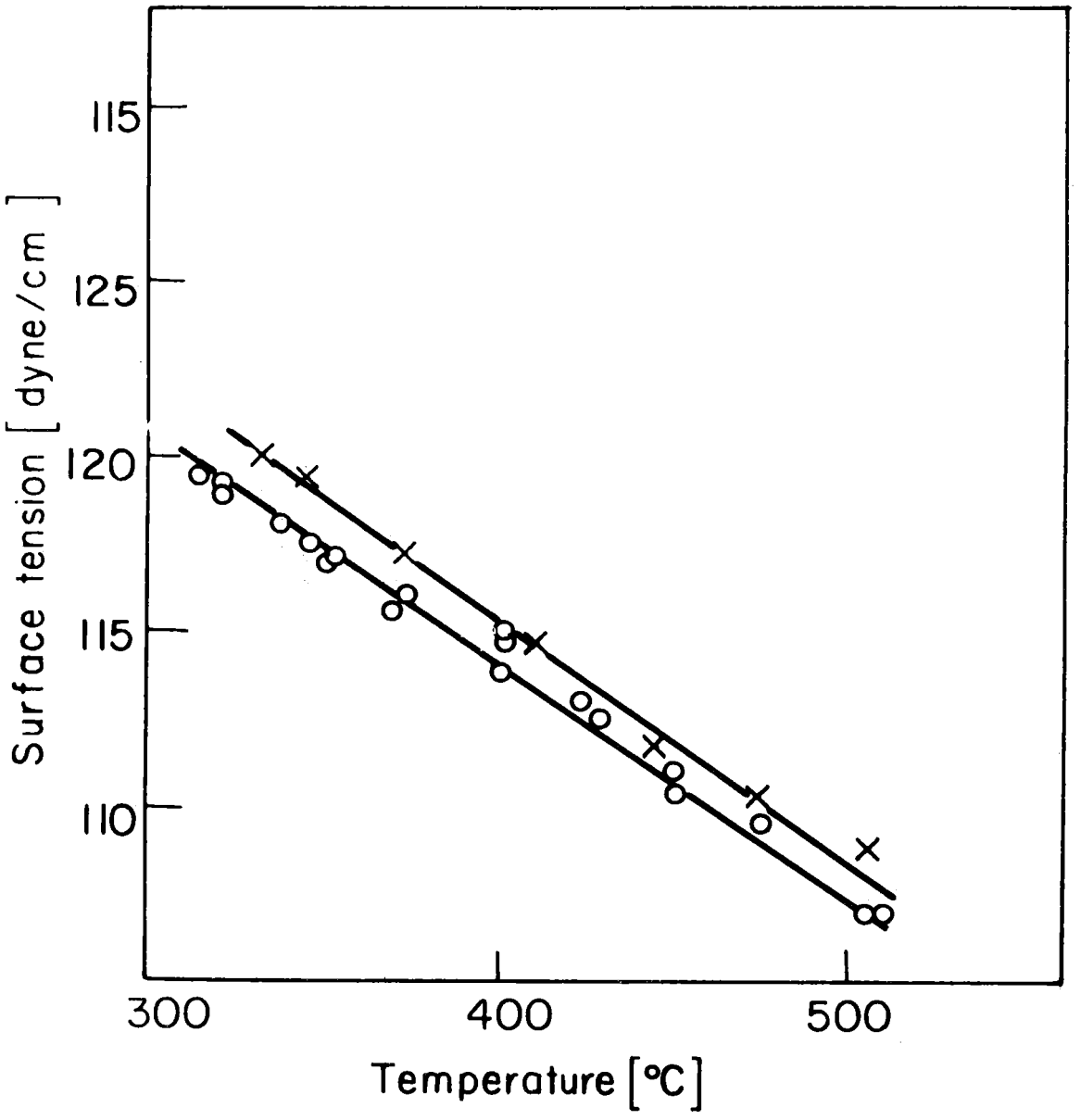

Figure 9. Surface Tension of Molten Sodium Nitrate. o: Dahl and Duke[11]; x: this work

Techniques of Measurements

Surface tension, density and viscosity measurements--Previous surface tension measurements made by the photographic sessile drop method are reported elsewhere [12,13]. Because of the small size of the drop and the large size of the chamber, vaporization of salt, pickup of contaminants and similar problems reduced the accuracy of the measurements. Present studies showed that the sessile drop results were approximately 2-5% too low.

The need for better surface tension results than those obtained with the sessile drop method led to the development of the pull-plate method described above. All subsequent measurements of surface tension, density, and viscosity were, therefore, made in the same apparatus merely by changing the immersed body as appropriate to the particular quantity being measured.

Contact angle measurements--Measurements of contact angle were carried out using a single-drop quartz cell, mounted in a horizontal furnace, which could be operated under vacuum or under a controlled atmosphere.

An optical or a photographic system similar to that described in the literature [12,13] was used. Drops were photographed in a parallel beam of light, using a 3000 Polaroid film. As a source of light, a 100 watt arc lamp was used. The furnace was connected to a rotary pump and a single stage glass mercury diffusion pump. The pressure of the system was measured by an ion gauge head and RG-21X Type control unit.

Preparation of the Melts and Sessile Drop Substrates

"Baker Analyzed" Reagent lithium chloride and lithium carbonate were used. Lithium chloride was dried in a slow flow of dry argon under pressure of 100-200μ. Argon was dried by passing through Linde molecular sieve Type 4A size 1/16 PLTS obtained from Union Carbide Corp. The drying temperature was gradually increased from room temperature to about 450°C in intervals of 60°C over 30 hours. Lithium carbonate was treated in the same way, but using CO_2 instead of argon. Dried salts were stored in a VAC Dry-Lab under argon.

Melts were prepared in a dry-box. A gold-palladium crucible was used. Mixtures of salts were fused under CO_2 atmosphere and were then crushed and stored in a dry-box.

The solid substrates (e.g., stainless steel 304, 316 and 347) were cut in pieces of 1.5×1.5 cm^2, squared at the edges, and then polished with alumina polishing powder. Before use, the substrates were degreased with organic solvents, washed with distilled water, and then finally dried in vacuo in the sessile drop cell at 200°C or above. The graphite substrates (spectroscopically

pure graphite grade AGKS from Union Carbide Corp., and graphite POCO porous AX from Pure Carbon Co.) were cut in pieces of 2.0×2.0 cm^2, carefully polished until a flat surface was obtained. The cut pieces were boiled in concentrated hydrochloric acid, and then in distilled water, dried at 140°C, and vacuum desiccated at 500°C.* The ceramic samples, recrystallized alumina and AlN, were washed with organic solvents and distilled water and heated to about 1000°C in a stream of dried oxygen, for the first, and of dried nitrogen, for the second ceramics.

Procedure of Measurements

Surface tension, density and viscosity measurements--Due to the different weights of the bob, viscometer plate and the plate for surface tension measurements, it is necessary to adjust the position of the core. This is achieved by means of the modified Delmar stopcock located at the top of the spring case. With the stopcock a position is found for zero output of LVDT. To ensure free movement of the bob, the whole system has to be aligned. The alignment is performed by means of a mirror under direct observation of a beam of light through the gap between the core and the transducer housing. The alignment is achieved by adjustment of the clamps that support the system. To check this visual setting, the system is set in oscillation by applying a momentary d.c. pulse to one of the secondary windings of LVDT, and oscillations signals are recorded. A dissymmetry of the oscillations indicates that the core is not properly located.

To charge a sample, the furnace was lowered by means of two big jacks. Then, the crucible assembly is removed from the furnace, and the crucible is cleaned, dried at 150°C and filled, in the dry-box, with the appropriate salt. The amount of a salt is determined so that a level required for an experiment is obtained (e.g., for viscosity and density measurements, it is necessary to cover completely the bob or the plate). For surface tension measurements, one centimeter depth of liquid would be sufficient. However, it is better to use more salt because: a) it will act as heat capacitor, and b) any change in the composition due to volatilization of LiCl or to decomposition of Li_2CO_3 will be minimized. Once the crucible has been placed into the furnace, the temperature is gradually increased while a suitable atmosphere is maintained by passing CO_2 into the bottom inlet of the crucible assembly.

For density measurements, the output of LVDT with the bob suspended in air is recorded at room temperature and again at working temperature. After the desired temperature is reached, the crucible is carefully raised by means of the Delmar stopcock

*Cf. reference 14.

(see above) until the bob reaches the level of the melt as indicated by a sudden jump of the LVDT output. Further rise of the crucible decreases the output until the bob is completely immersed. The output of LVDT is then almost unaffected by crucible position. Thus, a rise of 10 mm, for the wire used in these expermiments, produces a change in the output of only 0.04 mV when the density of the liquid is 1.7 g/cm^3. The difference between the last reading and that in air gives the buoyancy. Outputs are read on a Keithley 660 Differential Voltmeter.

For surface tension measurements, the output of LVDT with the plate in air is recorded at working temperature. A recorder (Sargent Recorder Model SR) is used for these measurements. The crucible is raised until the melt touches the plate. The point of contact is detected as a sharp increase in the output of LVDT. The crucible is, then, very slowly lowered while the output continues to increase until it reaches a maximum. The difference in the outputs for the plate in air and that when the maximum occurs gives the corresponding pull on the plate due to the surface forces.

For viscosity measurements, when a plate is completely immersed into the melt and working temperature set up, the system is set in oscillation by applying a small d.c. pulse on one of the secondary windings of the transducer, and the resulting output of the transducer is recorded (Esterline-Angus Speed Servo recorder, Model 850 X93). The amplitudes of the oscillations are then measured, and from this the logarithmic decrement is obtained.

Contact angle measurements--For sessile drop measurements, the operating technique used is simple. The sessile drop cell is cleaned with distilled water and dried at about 150°C. The cell is then introduced into a dry-box in which the substrate plate with a solid fragment of salt on it is placed on the sample platform of the cell. After removing from the dry-box the cell is located on the optical bench and attached to the vacuum line. The system is then evacuated and outgassed for one hour at a temperature of about 400°C. CO_2 is then introduced into the cell and the appropriate temperature is set up. Temperature measurements are made with a chromel-alumel thermocouple set below the sample platform.

For each experiment a magnification measurement is made by taking a photograph of a steel ball bearing of known size. From photographs, the values of γ and θ may be calculated by methods described elsewhere [12,13,15,16]. Values of θ can also be measured directly from the photograph. The dimensions of the drops were measured from the photographs using a caliper.

RESULTS

Viscosity

Logarithmic decrements and viscosities obtained for the LiCl-Li_2CO_3 system are summarized in Tables 8-14. Seven different concentrations are examined. The dependence of viscosity on temperature is shown in Figure 10 for all seven concentrations. An inspection of the figure shows that log viscosity is a linear function of 1/T, and hence the viscosity can be related to temperature by the Arrhenius expression:

$$\eta = \eta_0 \exp(E_{vis}/RT)$$

The activation energy for the viscous flow can now be recalculated as

$$E_{vis} = 4.576 \times \frac{d \log \eta}{d(1/T)}$$

where $d \log \eta/d(1/T)$ is the slope in $\log \eta$-(1/T) curves. This slope increases gradually with concentration of Li_2CO_3. In Figure 11, calculated values of the activation energy are plotted versus mole percent of Li_2CO_3.

Viscosity changes gradually with the composition of melts. Figure 12 gives the dependence of viscosity at 740°C on melt composition. In this figure, data for pure molten salts are included [6,7].

Surface Tension

The data on surface tension measurements for LiCl-Li_2CO_3 melts are summarized in Tables 15-20. Temperature dependence of surface tension is shown in Figure 13. In the same figure, values for the pure compounds are included [6,18]. At all compositions, surface tension of melts can be expressed as a linear function of temperature. Equations of the form $\gamma = a - b \times 10^{-3}t$ were deduced. Here, t is temperature in °C. Values for a and b are given in Table 21. The accuracy of the method was found to be ± 0.2 dyne cm^{-1}. Surface tension composition isotherms are given in Figure 14.

Surface tension data of melts in which Li_2O is dissolved into LiCl-Li_2CO_3 mixtures are also obtained in the present work. The following mole compositions are examined: 6.5:65.4:28.1 and 10:70:20, in the order Li_2O, LiCl and Li_2CO_3. Results are collected in Tables 22 and 23. There is a large increase in the surface tension with the addition of 6.5% Li_2O, and then an even bigger decrease with 10% Li_2O. (Since only two solutions are used, the surface tension versus percent Li_2O isotherms are not given.) These solutions were highly corrosive; the gold-palladium

TABLE 8. VICSOSITY OF LiCl (90 mole %) - Li_2CO_3 (10 mole %)

Temp. (°C)	Temp. (°K)	Density ρ (g/cm^3)	Logarithmic Decrement, δ	Area Correction A	η (Centipoises)
584	857	1.5492	0.04651	1.0184	2.060
607	880	1.5393	0.04480	1.0191	1.921
626	899	1.5311	0.04358	1.0198	1.825
644	917	1.5233	0.04208	1.0204	1.708
664	937	1.5149	0.04095	1.0210	1.624
681	954	1.5077	0.04002	1.0216	1.556
699	972	1.5001	0.03914	1.0222	1.494
721	994	1.4908	0.03792	1.0229	1.409
747	1020	1.4797	0.03633	1.0238	1.300

TABLE 9. VISCOSITY OF LiCl (85 mole %) - Li_2CO_3 (15 mole %)

Temp. (°C)	Temp. (°K)	Density ρ (g/cm^3)	Logarithmic Decrement, δ	Area Correction A	η (Centipoises)
577	850	1.5691	0.05087	1.0182	2.436
595	868	1.5616	0.04923	1.0187	2.289
617	890	1.5523	0.04732	1.0195	2.124
636	909	1.5445	0.04600	1.0201	2.015
668	941	1.5311	0.04319	1.0202	1.787
699	972	1.5181	0.04102	1.0222	1.622
722	995	1.5084	0.03962	1.0229	1.521
749	1022	1.4971	0.03805	1.0238	1.410

TABLE 10. VISCOSITY OF LiCl (80 mole %) - Li_2CO_3 (20 mole %)

Temp. (°C)	Temp. (°K)	Density ρ (g/cm^3)	Logarithmic Decrement, δ	Area Correction A	η (Centipoises)
564	837	1.5910	0.05818	1.0177	3.147
582	855	1.5837	0.05591	1.0183	2.915
605	878	1.5745	0.05307	1.0191	2.638
628	901	1.5653	0.05099	1.0198	2.445
650	923	1.5567	0.04893	1.0206	2.260
668	941	1.5494	0.04726	1.0212	2.116
690	963	1.5405	0.04562	1.0219	1.980
721	994	1.5281	0.04364	1.0229	1.822
745	1018	1.5185	0.04208	1.0237	1.702

TABLE 11. VISCOSITY OF LiCl (70 mole %) - Li_2CO_3 (30 mole %)

Temp. (°C)	Temp. (°K)	Density ρ (g/cm^3)	Logarithmic Decrement, δ	Area Correction A	η (Centipoises)
552	825	1.6645	0.07037	1.0173	4.407
565	838	1.6600	0.06802	1.0178	4.198
585	858	1.6520	0.06409	1.0184	3.674
606	879	1.6453	0.06142	1.0191	3.383
621	894	1.6400	0.05973	1.0196	3.206
639	912	1.6332	0.05756	1.0202	2.986
670	943	1.6220	0.05401	1.0212	2.641
696	969	1.6123	0.05171	1.0221	2.431
726	999	1.6015	0.04936	1.0231	2.225

TABLE 12. VISCOSITY OF LiCl (60 mole %) - Li_2CO_3 (40 mole %)

Temp. (°C)	Temp. (°K)	Density ρ (g/cm^3)	Logarithmic Decrement, δ	Area Correction A	η (Centipoises)
598	871	1.6822	0.07180	1.0188	4.526
615	898	1.6758	0.06888	1.0194	4.176
636	909	1.6682	0.06597	1.0201	3.843
654	927	1.6617	0.06335	1.0207	3.553
674	947	1.6543	0.06099	1.0214	3.303
689	962	1.6488	0.05890	1.0219	3.087
726	999	1.6353	0.05626	1.0231	2.832
747	1020	1.6277	0.05395	1.0238	2.613

TABLE 13. VISCOSITY OF LiCl (50 mole %) - Li_2CO_3 (50 mole %)

Temp. (°C)	Temp. (°K)	Density ρ (g/cm^3)	Logarithmic Decrement, δ	Area Correction A	η (Centipoises)
619	892	1.6922	0.07628	1.0195	5.072
636	909	1.6850	0.07301	1.0201	4.661
655	928	1.6771	0.07012	1.0207	4.314
674	947	1.6692	0.06797	1.0214	4.067
697	970	1.6596	0.06477	1.0221	3.708
719	992	1.6503	0.06212	1.0228	3.425
747	1020	1.6387	0.05896	1.0238	3.101

TABLE 14. VISCOSITY OF LiCl (30 mole %) - Li_2CO_3 (70 mole %)

Temp. (°C)	Temp. (°K)	Density ρ (g/cm^3)	Logarithmic Decrement, δ	Area Correction A	η (Centipoises)
694	967	1.7417	0.07913	1.0220	5.278
716	989	1.7327	0.07577	1.0227	4.864
735	1008	1.7249	0.07282	1.0234	4.501
756	1026	1.7162	0.07012	1.0241	4.188

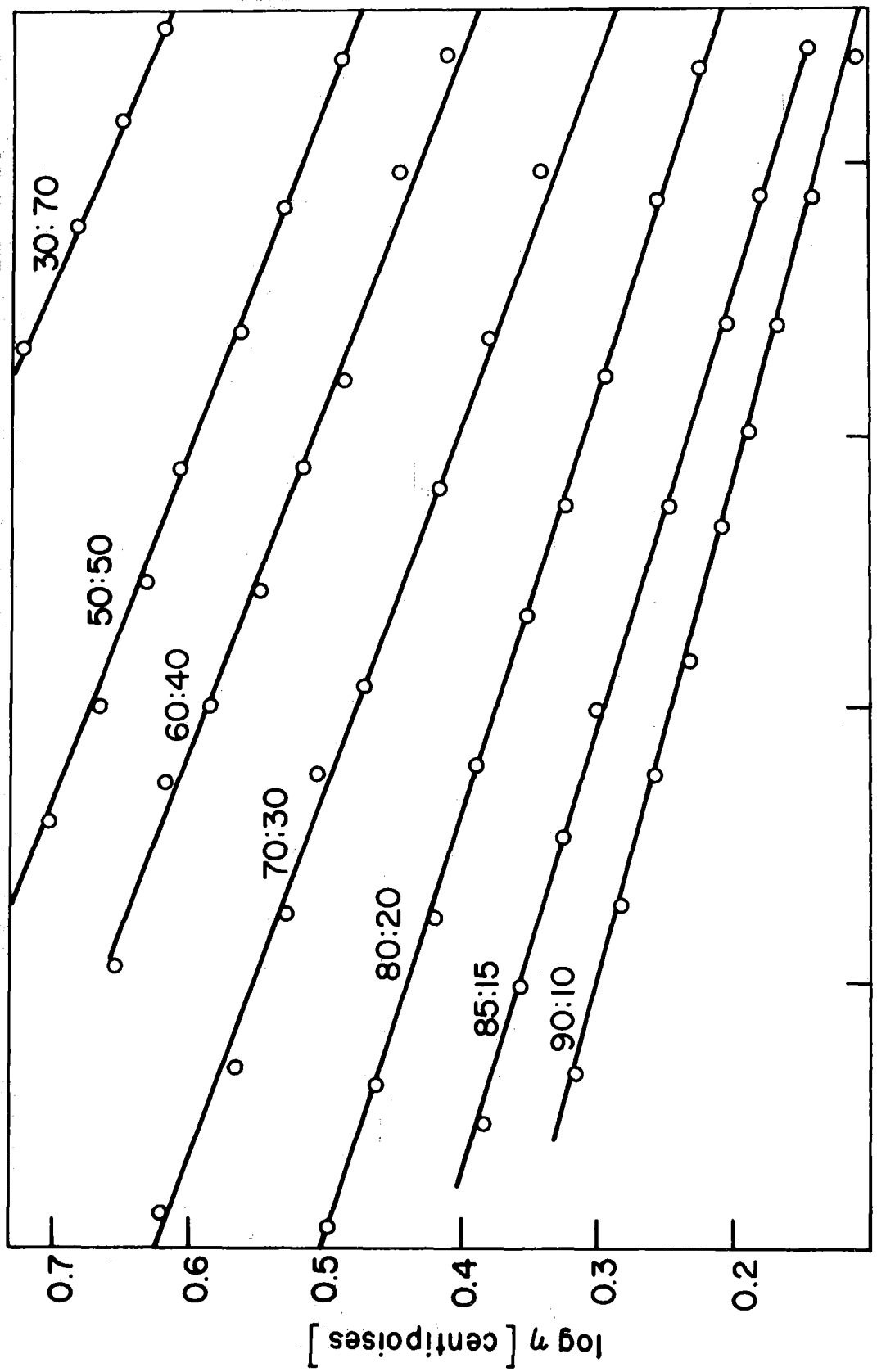

Figure 10. Viscosity vs. Reciprocal Temperature for $LiCl-Li_2CO_3$

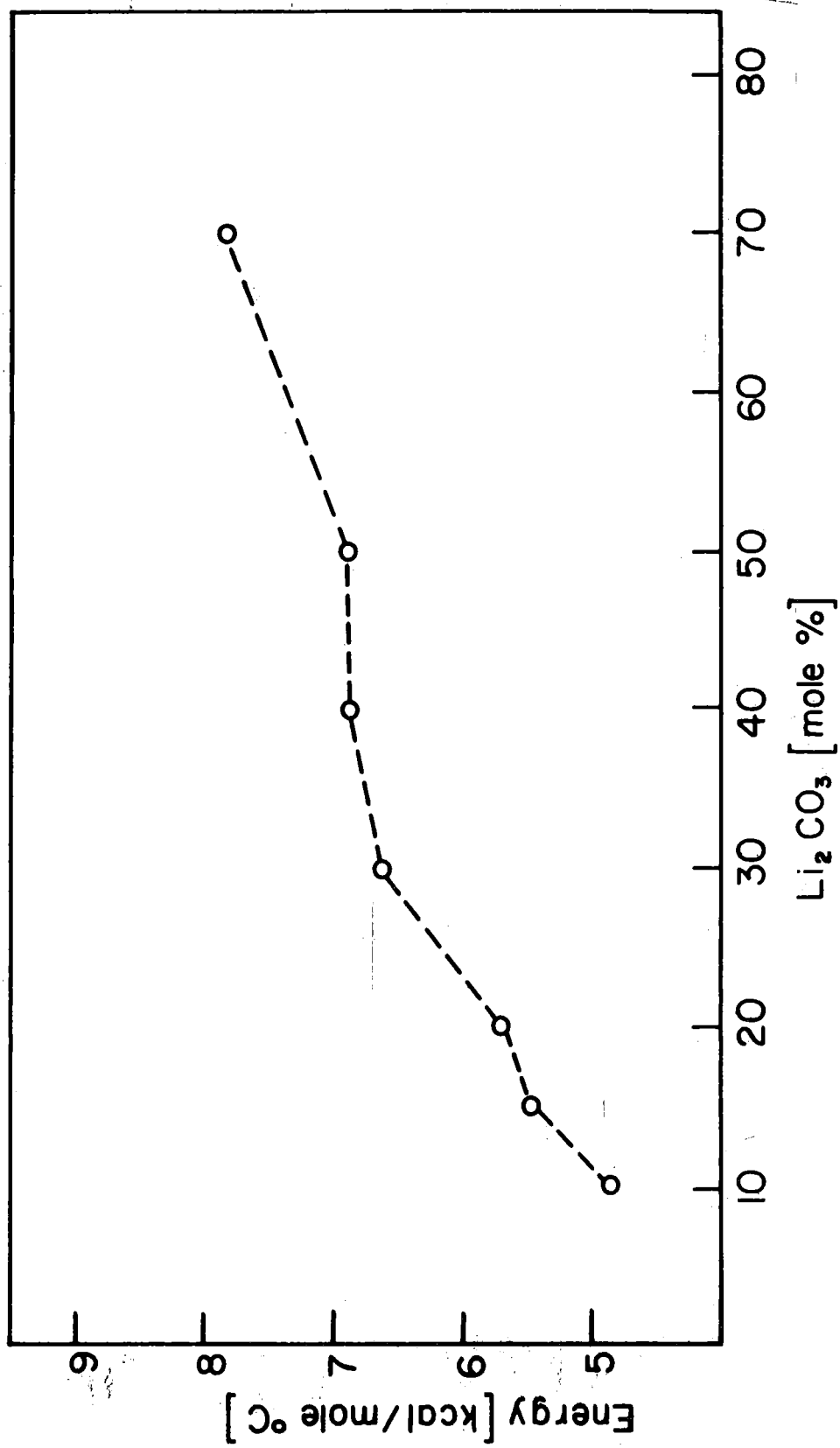

Figure 11. Activation Energy (viscosity) Versus Composition

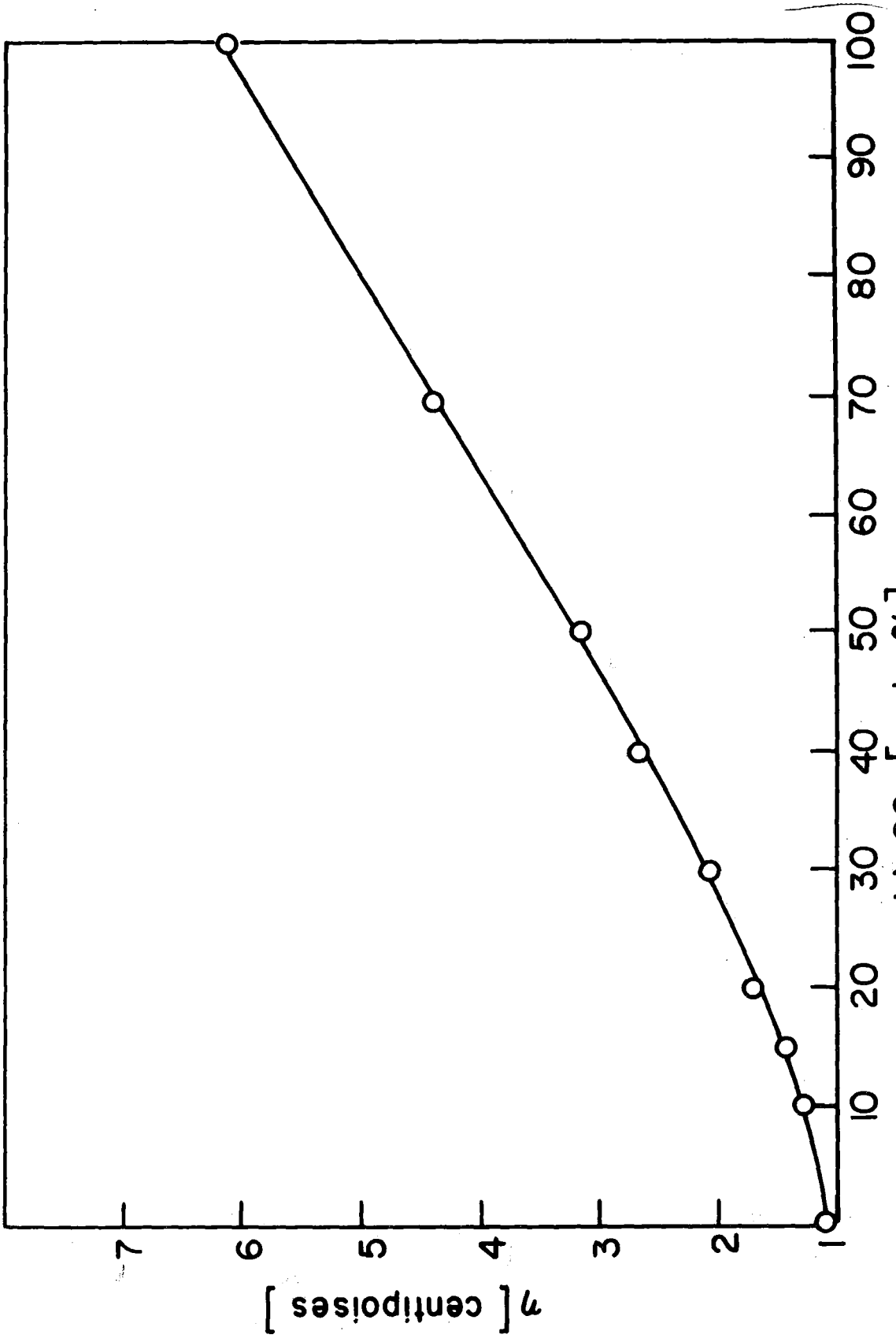

Figure 12. Viscosity Versus Composition at 740°C

TABLE 15. SURFACE TENSION OF LiCl (90 mole %) - Li_2CO_3 (10 mole %)

Temp. (°C)	Maximum Pull W (mV)	Maximum Pull W (grams)	Plate Perimeter (cm)	Surface Tension (dynes/cm)
565	26.83	0.16134	1.1142	142.1
590	26.66	0.16032	1.1146	141.1
606	26.53	0.15954	1.1149	140.4
621	26.37	0.15857	1.1152	139.5
655	26.00	0.15635	1.1158	137.5
681	25.50	0.15334	1.1162	134.8
713	25.22	0.15166	1.1168	133.2
745	24.86	0.14949	1.1173	131.3

TABLE 16. SURFACE TENSION OF LiCl (80 mole %) - Li_2CO_3 (20 mole %)

Temp. (°C)	Maximum Pull W (mV)	Maximum Pull W (grams)	Plate Perimeter (cm)	Surface Tension (dynes/cm)
553	28.43	0.17096	1.1325	148.1
575	28.23	0.16976	1.1391	147.0
601	27.81	0.16723	1.1334	144.8
623	27.63	0.16615	1.1338	143.8
644	27.40	0.16477	1.1341	142.5
663	27.35	0.16447	1.1345	142.2
683	26.99	0.16230	1.1348	140.3
702	26.85	0.16146	1.1352	139.5
718	26.81	0.16122	1.1355	139.3
735	26.45	0.15906	1.1358	137.4
754	26.35	0.15845	1.1361	136.8

TABLE 17. SURFACE TENSION OF LiCl (70 mole %) - Li_2CO_3 (30 mole %)

Temp. (°C)	Maximum Pull W (mV)	Maximum Pull W (grams)	Plate Perimeter (cm)	Surface Tension (dynes/cm)
537	30.55	0.18371	1.1322	159.2
557	30.35	0.18251	1.1332	158.1
591	29.80	0.17920	1.1332	155.1
594	29.85	0.17950	1.1333	155.4
613	29.75	0.17890	1.1336	154.8
613	29.73	0.17878	1.1336	154.7
645	29.30	0.17619	1.1338	152.4
678	28.98	0.17424	1.1347	150.6
699	28.92	0.17394	1.1351	150.3
740	28.47	0.17120	1.1359	147.9

TABLE 18. SURFACE TENSION OF LiCl (60 mole %) - Li_2CO_3 (40 mole %)

Temp. (°C)	Maximum Pull W (mV)	Maximum Pull W (grams)	Plate Perimeter (cm)	Surface Tension (dynes/cm)
610	30.77	0.18503	1.1150	162.8
624	30.65	0.18431	1.1152	162.1
644	30.50	0.18341	1.1156	161.3
662	30.38	0.18269	1.1159	160.6
675	30.26	0.18197	1.1161	159.9
700	30.02	0.18052	1.1165	158.6
745	29.65	0.17830	1.1173	156.5

TABLE 19. SURFACE TENSION OF LiCl (50 mole %) - Li_2CO_3 (50 mole %)

Temp. (°C)	Maximum Pull W (mV)	Maximum Pull W (grams)	Plate Perimeter (cm)	Surface Tension (dynes/cm)
648	33.02	0.19856	1.1342	171.7
675	32.72	0.19676	1.1347	170.1
706	32.25	0.19393	1.1352	167.6
736	31.81	0.19129	1.1358	165.2
751	31.68	0.19051	1.1361	164.5
769	31.35	0.18852	1.1364	162.7

TABLE 20. SURFACE TENSION OF LiCl (30 mole %) - Li_2CO_3 (70 mole %)

Temp. (°C)	Maximum Pull W (mV)	Maximum Pull W (grams)	Plate Perimeter (cm)	Surface Tension (dynes/cm)
679	36.35	0.21859	1.1162	192.1
703	36.16	0.21745	1.1166	191.0
704	36.15	0.21739	1.1166	191.0
722	36.03	0.21666	1.1169	190.3
738	35.95	0.21618	1.1172	189.8
760	35.82	0.21540	1.1176	189.1
776	35.68	0.21456	1.1179	188.3

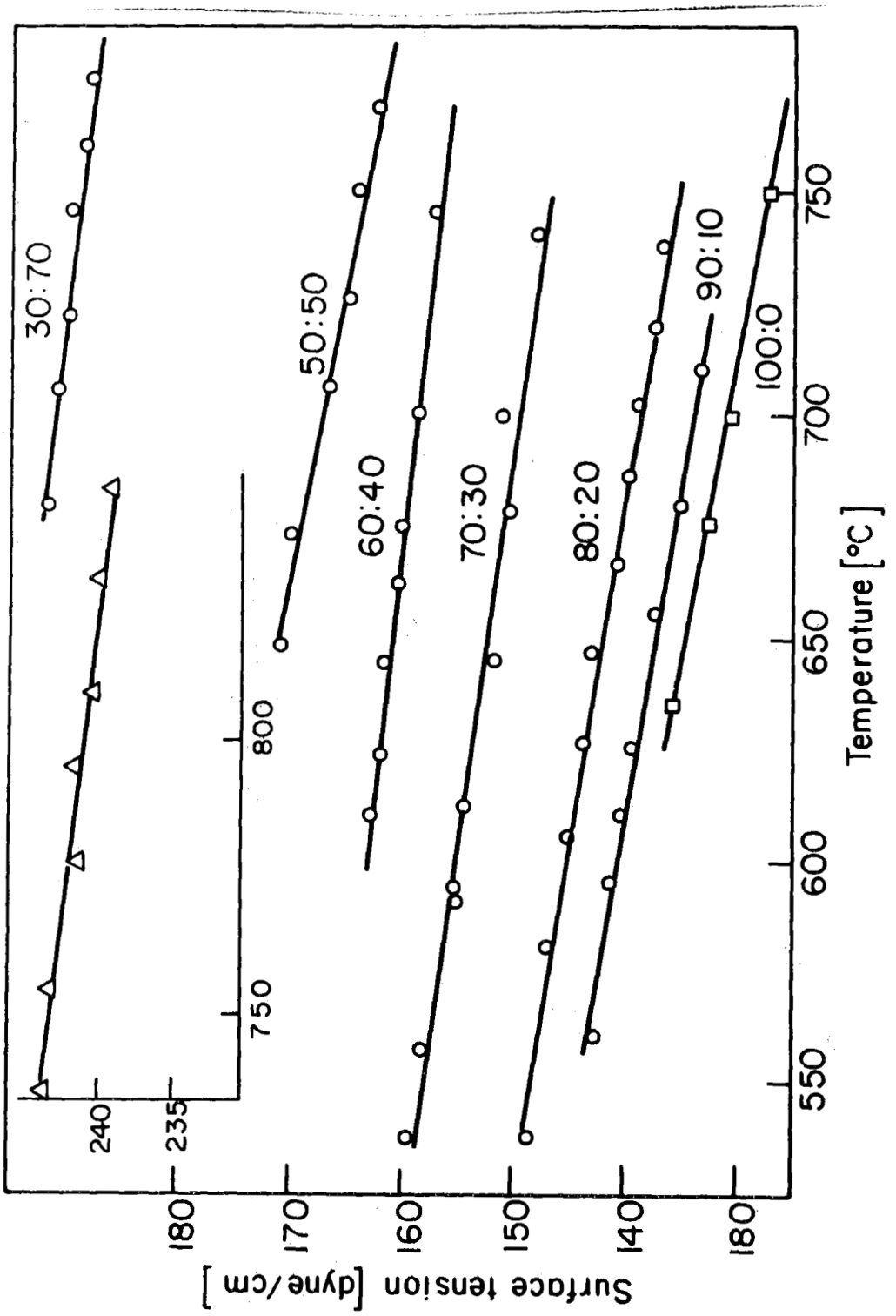

Figure 13. Surface Tension of LiCl: Li_2CO_3 Melts. o: this work; Δ: Li_2CO_3 (Janz and Lorenz[8]); □: LiCl (Janz[6])

TABLE 21. PARAMETERS FOR SURFACE TENSION EQUATION

Composition Mole % LiCl	a	b
100	180.5	0.071
90	180.5	0.058
80	185	0.057
70	189	0.057
60	192	0.048
50	216	0.075
30	216	0.036
0	273	0.04

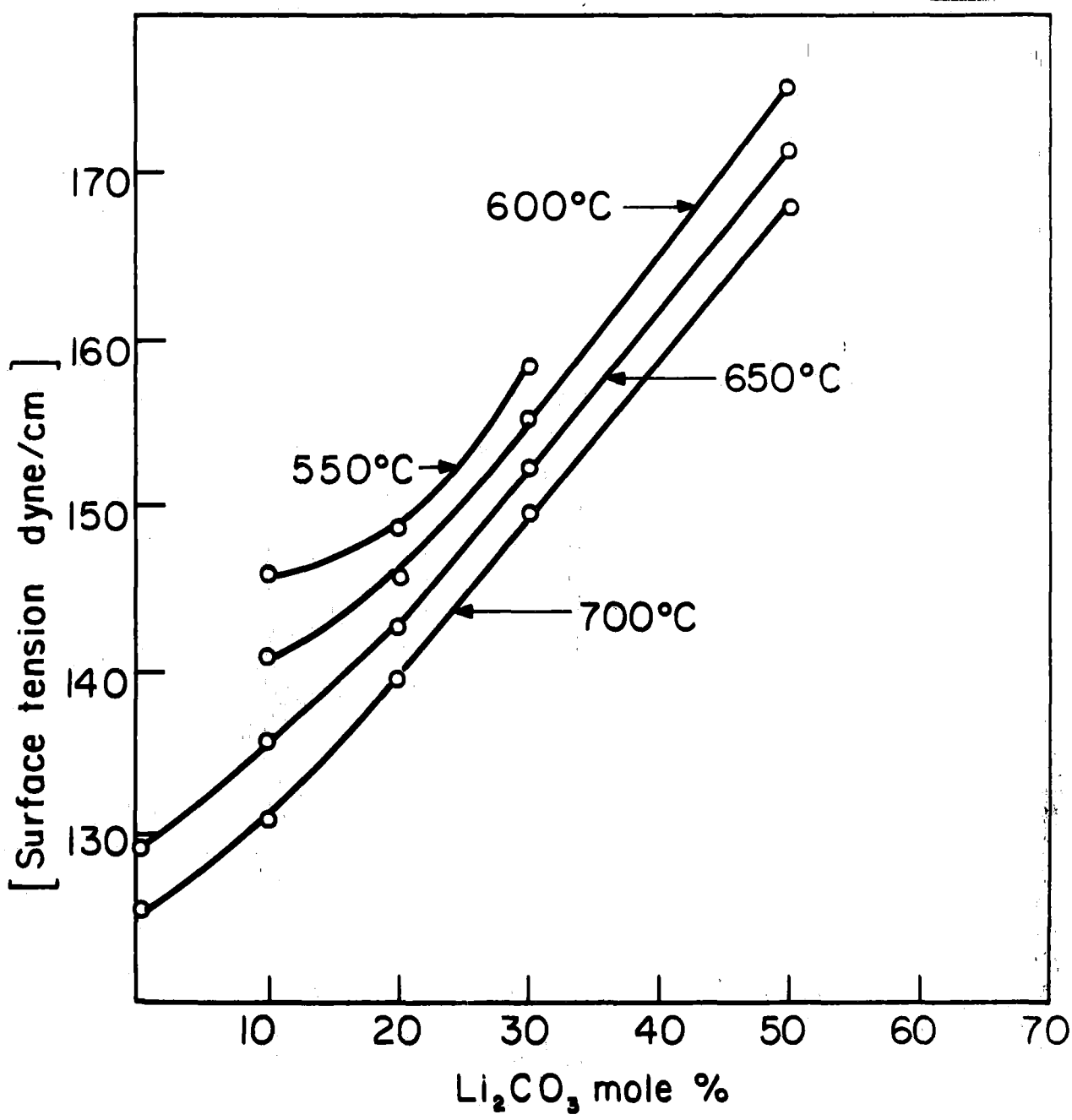

Figure 14. Surface Tension Versus Concentration. LiCl-Li_2CO_3

TABLE 22. SURFACE TENSION OF LiCl (65.4 mole %) - Li_2O (6.5 mole %) - Li_2CO_3 (28.1 mole %)

Temp. (°C)	Maximum Pull W (mV)	Maximum Pull W (grams)	Plate Perimeter (cm)	Surface Tension (dynes/cm)
559	31.40	0.18882	1.1326	163.5
583	31.12	0.18714	1.1331	162.0
601	30.93	0.18600	1.1334	161.0
623	30.85	0.18551	1.1338	160.5
654	30.60	0.18401	1.1343	159.1
687	30.12	0.18112	1.1349	156.6

TABLE 23. SURFACE TENSION OF LiCl (70 mole %) - Li_2O (10 mole %) - Li_2CO_3 (20 mole %)

Temp. (°C)	Maximum Pull W (mV)	Maximum Pull W (grams)	Plate Perimeter (cm)	Surface Tension (dynes/cm)
579	29.16	0.17535	1.1144	154.4
598	29.01	0.17445	1.1148	153.5
634	28.65	0.17228	1.1154	151.5
667	28.08	0.16886	1.1160	148.4

alloy crucible developed a golden surface color, and the melt became blue-gray.

Densities

The values of density obtained in the present work for LiCl-Li_2CO_3 melts, and values of surface tension used to account for the surface tension effects on the suspension wire are given in Tables 24-31. The variation of density with temperature was found to be linear (Fig. 15). The equation $\rho = \rho_0 - bt$ expresses this linearity.

Contact Angle

Experiments on wetting behavior of the molten mixtures of LiCl-Li_2CO_3 were performed on substrates of Al_2O_3, AlN, stainless steel 316, 304 and 347, graphite POCO AX and spectroscopically pure graphite in CO_2 atmosphere. With the exception of POCO graphite and spectroscopically pure graphite, the substrates were completely wetted by liquid salts. Present results are recorded in Tables 32-35. Table 36 shows the values of the contact angles obtained for pure LiCl. The dependence of contact angle upon temperature is shown in Figures 16, 17 and 18. It can be seen that in all cases the contact angle is nearly unaffected by temperature over the range from just above the melting point to nearly 800°C. There is only about an 8% change in θ, on POCO graphite substrate, from pure LiCl to 30:70 LiCl-Li_2CO_3 mixture (cf. Fig. 19).

ANALYSIS OF ERRORS

Surface Tension

The surface tension is given by the equation

$$\gamma = \frac{Wg}{L_0(1 + \alpha\Delta t)}$$

where g is the acceleration due to gravity, L_0 is the perimeter of the plate, α is the linear expansion coefficient for the gold-palladium alloy, and Δt is given by the difference in temperature at which the experiment was carried out and that at which the perimeter of the plate was measured.

In order to obtain the maximum error in γ, the differential method was applied to the above equation:

$$\Delta\gamma = \frac{\partial\gamma}{\partial W}\Delta W + \frac{\partial\gamma}{\partial L}\Delta L + \frac{\partial\gamma}{\partial\alpha}\Delta\alpha + \frac{\partial\gamma}{\partial(\Delta t)}\Delta(\Delta t)$$

The maximum error was calculated for a typical measurement on a LiCl 80 mole %-Li_2CO_3 20 mole % melt at 623°C. The values of γ and the maximum probable error in each measured quantity are:

TABLE 24. DENSITY OF LiCl (90 mole %)-Li_2CO_3 (10 mole %)

Temp. (°C)	Buoyancy B+v (Volts)	Buoyancy B+v (grams)	Surface Tension γ (dynes/cm)	Surface Tension Correction, A (grams)	Bob Volume V_T (cm^3)	Density (g/cm^3)
581	0.29647	1.7828	141.7	0.0063	1.1532	1.5515
599	0.29533	1.7760	140.6	0.0063	1.1541	1.5443
617	0.29406	1.7683	139.4	0.0063	1.1551	1.5364
638	0.29226	1.7575	138.1	0.0062	1.1562	1.5254
669	0.29002	1.7440	136.1	0.0061	1.1579	1.5115
695	0.28842	1.7344	134.4	0.0060	1.1593	1.5013
722	0.28679	1.7246	132.7	0.0059	1.1607	1.4909
748	0.38504	1.7141	131.1	0.0059	1.1621	1.4801

TABLE 25. DENSITY OF LiCl (80 mole %) - Li_2CO_3 (20 mole %)

Temp. (°C)	Buoyancy B+v (Volts)	Buoyancy B+v (grams)	Surface Tension γ (dynes/cm)	Surface Tension Correction, A (grams)	Bob Volume V_T (cm^3)	Density (g/cm^3)
562	0.30382	1.8270	147.8	0.0066	1.1521	1.5915
581	0.30227	1.8177	146.7	0.0066	1.1532	1.5820
598	0.30126	1.8116	145.7	0.0065	1.1541	1.5754
613	0.30044	1.8067	144.8	0.0065	1.1549	1.5700
643	0.29880	1.7968	143.1	0.0064	1.1565	1.5592
676	0.29700	1.7860	141.0	0.0063	1.1582	1.5474
700	0.29544	1.7766	139.7	0.0063	1.1595	1.5376
728	0.29359	1.7655	138.0	0.0062	1.1610	1.5260
752	0.29180	1754.7	136.5	0.0061	1.1623	1.5150

TABLE 26. DENSITY OF LiCl (74.8 mole %) - Li_2CO_3 (25.2 mole %)

Temp. (°C)	Buoyancy B+v (Volts)	Buoyancy B+v (grams)	Surface Tension γ (dynes/cm)	Surface Tension Correction, A (grams)	Bob Volume V_T (cm^3)	Density (g/cm^3)
569	0.31198	1.8761	151.9	0.0068	1.1525	1.6337
583	0.31183	1.8753	150.9	0.0068	1.1533	1.6319
618	0.30968	1.8623	148.7	0.0067	1.1551	1.6180
649	0.30833	1.8541	146.8	0.0066	1.1568	1.6085
683	0.30628	1.8418	144.6	0.0065	1.1586	1.5953
719	0.30408	1.8286	142.3	0.0064	1.1606	1.5811
755	0.30190	1.4155	139.8	0.0063	1.1625	1.5672

TABLE 27. DENSITY OF LiCl (70 mole %) - Li_2CO_3 (30 mole %)
(Test 1)

Temp. (°C)	Buoyancy B+v (Volts)	Buoyancy B+v (grams)	Surface Tension γ (dynes/cm)	Surface Tension Correction, A (grams)	Bob Volume V_T (cm^3)	Density (g/cm^3)
539	0.31778	1.9110	159.0	0.0071	1.1509	1.6666
548	0.31765	1.9102	158.5	0.0071	1.1514	1.6652
582	0.31613	1.9004	156.5	0.0070	1.1532	1.6540
604	0.31490	1.8937	155.2	0.0070	1.1544	1.6464
620	0.31419	1.8894	154.3	0.0069	1.1552	1.6415
648	0.31237	1.8784	152.6	0.0068	1.1567	1.6298
682	0.31044	1.8668	150.7	0.0068	1.1586	1.6171
708	0.30927	1.8598	149.1	0.0067	1.1599	1.6091

TABLE 28. DENSITY OF LiCl (70 mole %) - Li_2CO_3 (30 mole %)
(Test 2)

Temp. (°C)	Buoyancy B+v (Volts)	Buoyancy B+v (grams)	Surface Tension γ (dynes/cm)	Surface Tension Correction, A (grams)	Bob Volume V_T (cm^3)	Density (g/cm^3)
537	0.31709	1.9058	159.1	0.0071	1.1508	1.6631
541	0.31704	1.9065	158.9	0.0071	1.1510	1.6625
560	0.31635	1.9024	157.8	0.0071	1.1520	1.6575
580	0.31545	1.8970	156.6	0.0070	1.1531	1.6512
599	0.31425	1.8897	155.5	0.0070	1.1541	1.6435
657	0.31074	1.8686	152.1	0.0068	1.1572	1.6206
685	0.30904	1.8584	150.5	0.0067	1.1587	1.6096

TABLE 29. DENSITY OF LiCl (60 mole %) - Li_2CO_3 (40 mole %)

Temp. (°C)	Buoyancy B+v (Volts)	Buoyancy B+v (grams)	Surface Tension γ (dynes/cm)	Surface Tension Correction, A (grams)	Bob Volume V_T (cm^3)	Density (g/cm^3)
597	0.32196	1.9361	163.0	0.0073	1.1540	1.6840
610	0.32136	1.9325	162.8	0.0073	1.1547	1.6799
618	0.31999	1.9243	162.4	0.0073	1.1551	1.6722
630	0.31996	1.9241	161.8	0.0072	1.1558	1.6710
662	0.31776	1.9109	160.5	0.0072	1.1575	1.6571
695	0.31599	1.9002	158.9	0.0071	1.1593	1.6453
748	0.31324	1.8837	156.4	0.0070	1.1621	1.6269
772	0.31221	1.8775	155.3	0.0070	1.1634	1.6198

TABLE 30. DENSITY OF LiCl (50 mole %) - Li_2CO_3 (50 mole %)

Temp. (°C)	Buoyancy B+v (Volts)	Buoyancy B+v (grams)	Surface Tension γ (dynes/cm)	Surface Tension Correction, A (grams)	Bob Volume V_T (cm^3)	Density (g/cm^3)
636	0.32217	1.9374	172.8	0.0077	1.1561	1.6825
652	0.32147	1.9332	171.6	0.0077	1.1570	1.6775
669	0.32077	1.9290	170.3	0.0076	1.1579	1.6725
691	0.31971	1.9225	168.7	0.0076	1.1591	1.6653
705	0.31780	1.9105	167.3	0.0075	1.1598	1.6537
725	0.31647	1.9030	166.1	0.0074	1.1609	1.6457
744	0.31591	1.8997	164.7	0.0074	1.1619	1.6414

TABLE 31. DENSITY OF LiCl (29 mole %) - Li_2CO_3 (71 mole %)

Temp. (°C)	Buoyancy B+v (Volts)	Buoyancy B+v (grams)	Surface Tension γ (dynes/cm)	Surface Tension Correction, A (grams)	Bob Volume V_T (cm^3)	Density (g/cm^3)
690	0.33435	2.0106	191.6	0.0086	1.1590	1.7422
712	0.33320	2.0037	190.7	0.0085	1.1602	1.7344
732	0.33179	1.9952	189.9	0.0085	1.1612	1.7255
747	0.33090	1.9899	189.3	0.0085	1.1621	1.7197
764	0.32994	1.9841	188.6	0.0084	1.1630	1.7133

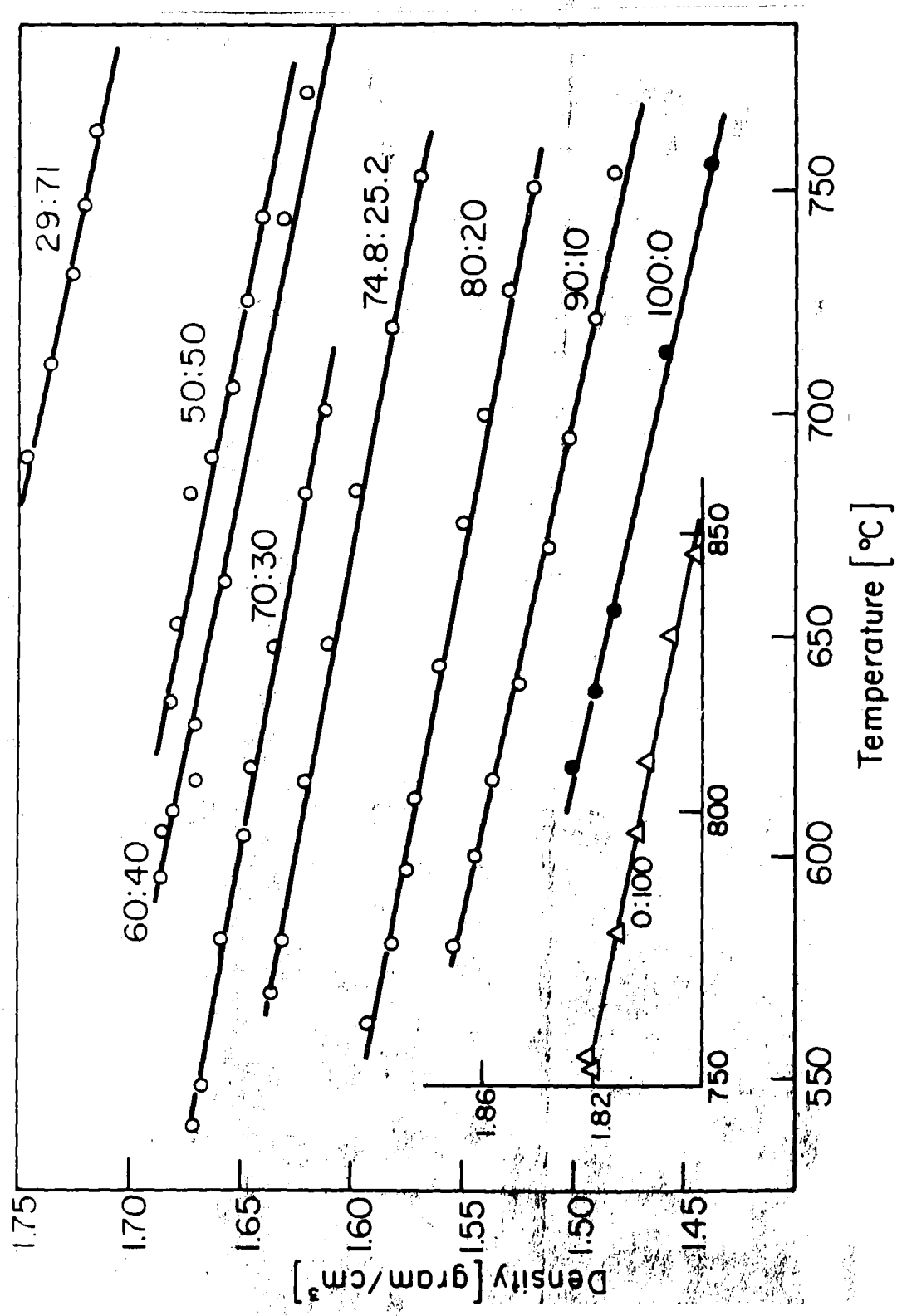

Density of Molten LiCl: Li_2CO_3 Mixtures. o: this work; LiCl (Van Artsdalen and Yaffe); Δ: Li_2CO_3 (Janz and Lorenz[8])

TABLE 32. CONTACT ANGLE OF LiCl (90 mole %) - Li_2CO_3 (10 mole %)

Substrate	θ	Temperature (°C)
Graphite POCO	149.6	576
" "	147.4	604
" "	149.8	631
" "	149.0	662
" "	147.2	720
" "	147.0	755
" "	148.1	787
Graphite Spectroscopic	143.6	571
" "	143.6	600
" "	142.0	627
" "	140.8	656
" "	143.8	684
" "	141.6	715
" "	141.4	784

TABLE 33. CONTACT ANGLE OF LiCl (70 mole %) - Li_2CO_3 (30 mole %)

Substrate	θ	Temperature (°C)
Graphite POCO	142.3	538
" "	139.7	567
" "	139.8	592
" "	142.2	632
" "	139.5	651
" "	139.9	705
" "	140.8	726
" "	140.8	773
Graphite Spectroscopic	134.3	536
" "	134.0	565
" "	134.2	603
" "	131.0	649
" "	129.2	699
" "	130.5	746

TABLE 34. CONTACT ANGLE OF LiCl (50 mole %) - Li_2CO_3 (50 mole %)

Substrate	θ	Temperature (°C)
Graphite POCO	139.7	627
" "	138.1	655
" "	139.2	685
" "	139.9	741
" "	138.6	765

TABLE 35. CONTACT ANGLE OF LiCl (30 mole %) - Li_2CO_3 (70 mole %)

Substrate	θ	Temperature (°C)
Graphite POCO	140.0	670
" "	141.5	697
" "	140.5	727
" "	140.7	754
" "	140.0	781

TABLE 36. CONTACT ANGLE OF PURE LiCl

Substrate	θ	Temperature (°C)
Graphite POCO	154.8	656
" "	150.8	656
" "	151.8	676
" "	149.8	686
" "	152.5	723
" "	153.3	723
" "	152.5	723
" "	150.8	728
" "	152.5	817
" "	152.4	817

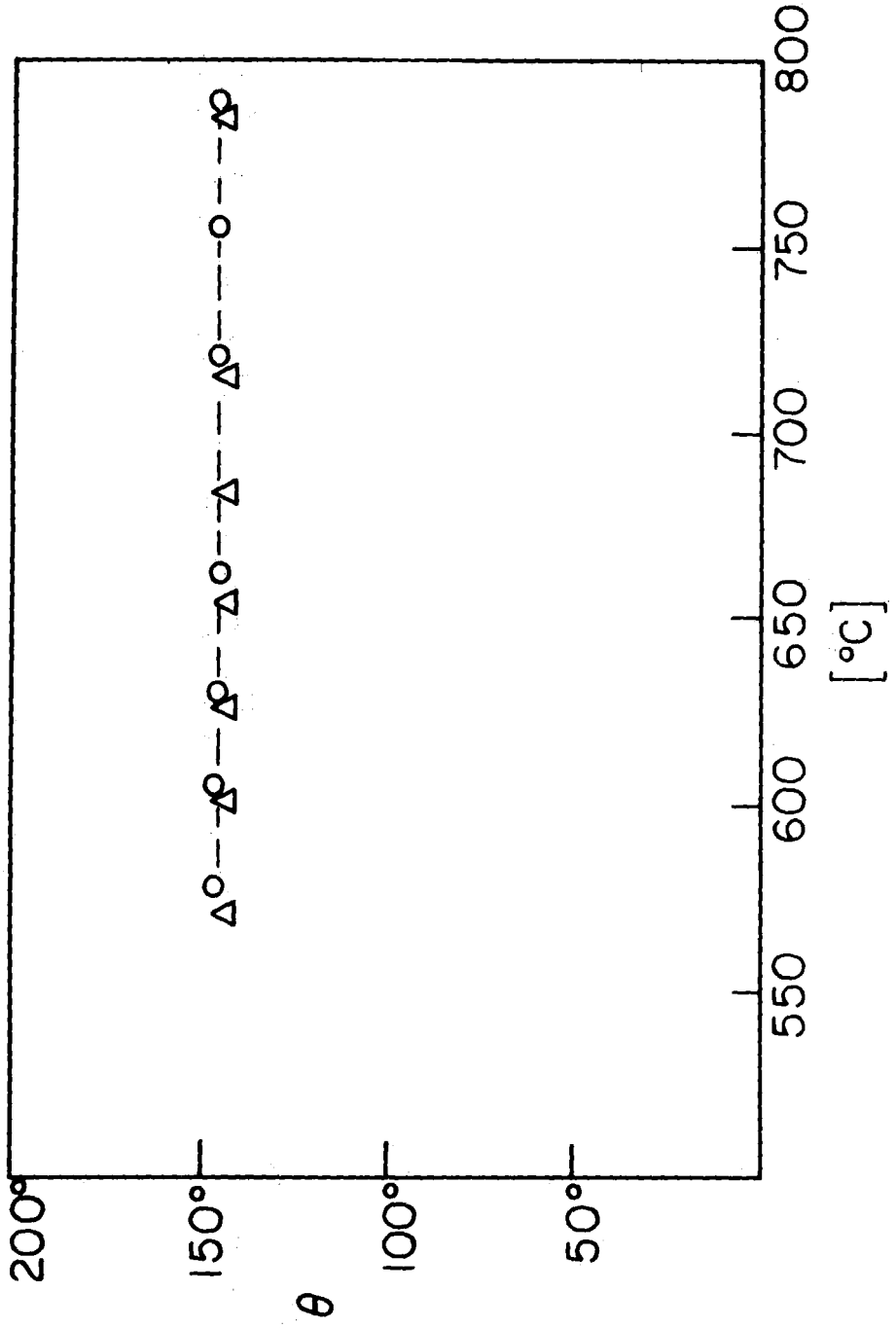

Figure 16. Contact Angle Versus Temperature. LiCl 90 Mole % - Li_2CO_3 10 Mole %; o: Graphite POCO; Δ: Spectroscopic Graphite

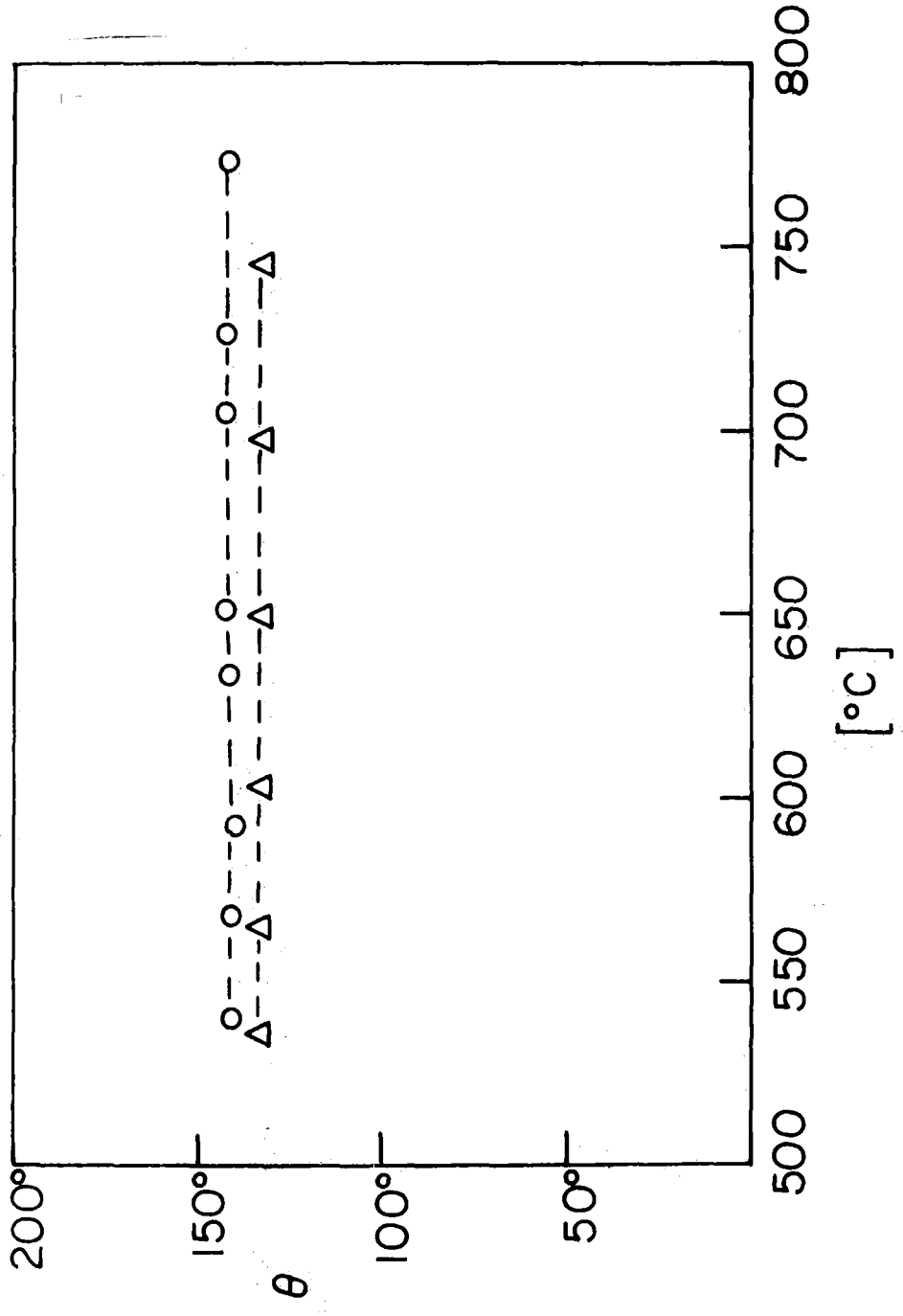

Figure 17. Contact Angle Versus Temperature. LiCl 70 Mole % - Li_2CO_3 30 Mole %; o: Graphite POCO; Δ: Spectroscopic Graphite

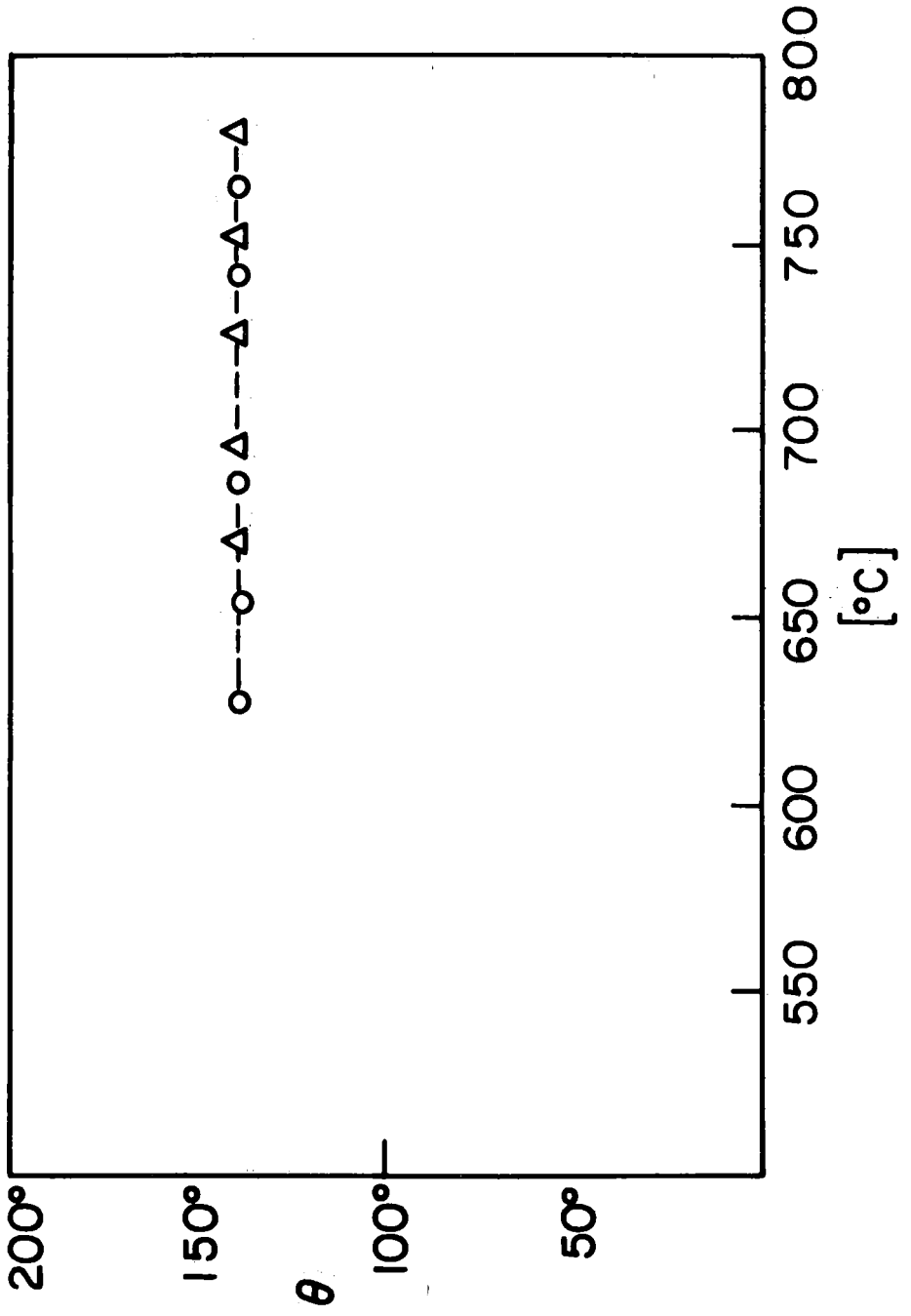

Figure 18. Contact Angle Versus Temperature. o : LiCl 50 Mole % - Li_2CO_3 50 Mole % on Graphite POCO; Δ : LiCl 30 Mole % - $LiCO_3$ 70 Mole % on Graphite POCO

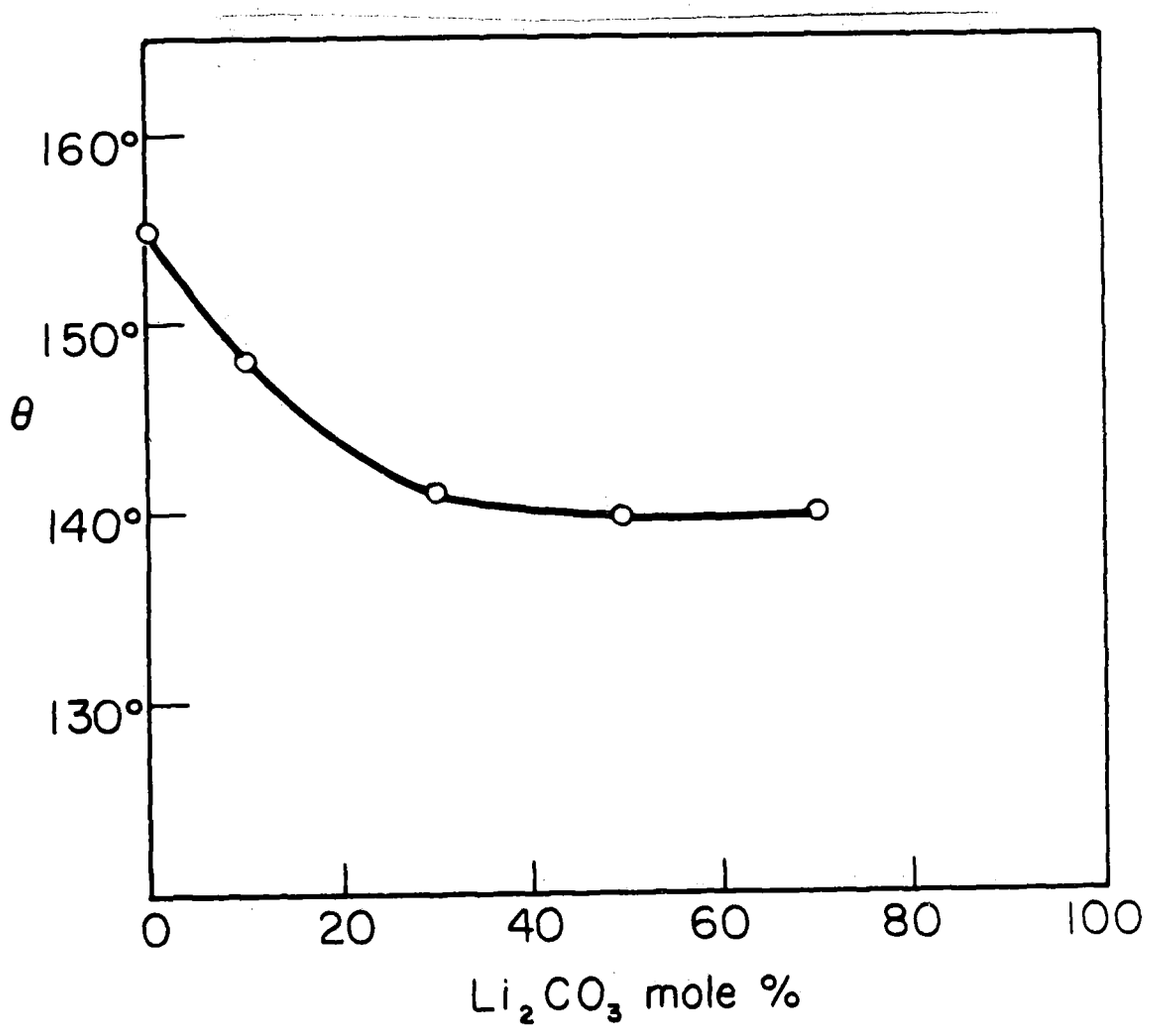

Figure 19. Contact Angle Versus Composition on Graphite POCO; (720°C)

γ = 143.8 dynes/cm

L_0 = 1.123 cm $\quad\quad$ ΔL = ±0.005 cm

W = 0.16615 g $\quad\quad$ ΔW = ±0.00018 g

Δt = 603°C $\quad\quad$ $\Delta(\Delta t)$ = ±1°C

$\alpha = 15.9\times10^{-6}$ cm/cm °C $\quad\quad$ $\Delta\alpha = \pm9.5\times10^{-7}$ cm/cm °C

From this set of values, $\Delta\gamma$ was found to be ±0.98 dynes/cm and the maximum relative error $\Delta\gamma/\gamma$ = ±0.007. The greatest contribution to $\Delta\gamma$ arises from the measurement of the perimeter of the plate, $(\partial\gamma/\partial L)\Delta L$ = 0.73 dyne/cm. The maximum error in α was estimated by Janz [6] to be about ±5%. The contribution to $\Delta\gamma$, for this case, is insignificant. The maximum probable error arising from the pull W was estimated from the accuracy of the measurement of the slope mg/mV; that was found to be ±0.0066 mg/mV.

There are two additional errors in the surface tension measurements. The first arises from the uncertainties in the temperature measurements, and the second from the uncertainties in the composition of the melts. The contribution to $\Delta\gamma$ due to the uncertainties in temperature was estimated to be ±0.03 dyne/cm, considering that the maximum error in the temperature was ±0.5°C, and the average temperature coefficient for the mixture is 0.060 dyne/cm °C.

The maximum error in the preparation of the melts was assumed to be 0.1 mole %, and considering that the maximum change of surface tension vs. composition is of the order of 1.2 dynes/cm for 1 mole %, the maximum error in γ turned out to be ±0.12 dynes/cm.

Thus, the total error in γ is ±1 dyne. Correspondingly, the reproducibility of the measurements was about ±0.2 dynes.

Density

The density is given by

$$\rho = \frac{B + v + A}{V_0(1 + 3\alpha t)}$$

where A, v, B, V_0, α and t are already defined. The application of the differential method to ρ gives:

$$\Delta\rho = \frac{\partial\rho}{\partial B}\Delta B + \frac{\partial\rho}{\partial v}\Delta v + \frac{\partial\rho}{\partial A}\Delta A + \frac{\partial\rho}{\partial V_0}\Delta V_0 + \frac{\partial\rho}{\partial\alpha}\Delta\alpha + \frac{\partial\rho}{\partial(\Delta t)}\Delta(\Delta t)$$

In order to calculate $\Delta\rho$, this equation was applied to a density measurement on a LiCl 80 mole %-Li_2CO_3 20 mole % melt at 598°C. The value of density together with the maximum errors are given below.

$\rho = 1.5754$ g/cm^3

$B = 1.8111$ g	$\Delta B = 0.0020$ g
$A = 0.0065$ g	$\Delta A = 0.00004$ g
$V_0 = 1.1541$ cm^3	$\Delta V_0 = 0.0005$ cm^3
$v = 0.0005$ g	$\Delta v = 0.00003$ g

From these values, $\Delta\rho$ was found to be ± 0.0030 g/cm^3 and the maximum relative error $\Delta\rho/\rho = \pm 0.0019$. The greatest contribution to $\Delta\rho$ arises from the error in the calibration of the LVDT (which affects the buoyancy, B). The slope mg/mv was found to be 6.0134 ± 0.0066. Thus, the buoyancy B is given with a maximum probable error of ± 0.0020 g, and therefore $(\partial\rho/\partial B)\Delta B = 0.0019$ g.

The volume of the bob V_0 does not include the same buoyancy error as that discussed above, because V_0 was measured with a balance (Mettler) and therefore the estimated maximum error on V_0 is much smaller than the error in measuring the buoyancy.

The error due to the surface tension correction is about five times smaller than that found by Janz [6]. The reason for this is that the diameter of the suspension wire used in the present work was five times smaller than that used by Janz. An advantage in using a thin wire is that there is no need to have the same depth of immersion of the bob because the contribution of the immersed suspension wire to the total buoyancy is insignificant. The errors involved in the temperature measurement and in the preparation of the mixtures were found to be, respectively, ± 0.0002 g/cm^3 and 0.0003 g/cm^3.

Viscosity

The viscosity was calculated by means of the equation

$$\eta = \frac{1538.29}{(1 + 2\alpha\Delta t)^2}(\delta^2 - 2.43\times10^{-4}\delta)$$

This equation was derived by applying the least square method to the results obtained on five organic solvents and molten potassium nitrate covering the range of temperatures from 347 to 471°C. The average standard relative error was found to be ± 0.01 for a viscosity of 2.777 centipoises. It is necessary to mention that the values of η and ρ used, obtained from the literature, may be less reliable than the logarithmic decrement obtained experimentally in the present work, owing to the rather large interpolation required. The error involved in density measurements only contributed ± 0.007 centipoises to the final error in viscosity. The contribution of α is insignificant due to the fact that the plate used in this case is made of pure gold and α has been well established. As the viscosity does not change in a linear way with

temperature, the maximum value of the slope η vs. T was taken in order to obtain the error in temperature measurement. It was found to be ±0.0008 centipoises. The error involved in preparation of the mixture was ±0.005 centipoises. Thus, the final error in viscosity will be of the order of ±1.5%.

COMPARISON WITH PREVIOUS WORK

Figure 11 shows the change of activation energy for viscous flow with composition. The activation energy is not a linear function of composition. A sharp change must occur close to the pure Li_2CO_3 side, for which the activation energy is reported [6] to be about 16 kcal/mole. The latter activation energy, therefore, falls to about 8 kcal/mole with the addition of 30 mole % LiCl to Li_2CO_3. From the composition 30 mole % LiCl to about 70 mole % LiCl, which percentage is close to the eutectoid composition, the activation energy remains nearly constant and close to 7 kcal/mole. At still higher concentration of LiCl, the activation energy again falls to reach about 4.9 kcal/mole at 90 mole % LiCl. The activation energy data for pure LiCl reported in the literature* are somewhat scattered, e.g., 5.0, 7.0, and 8.8 kcal/mole. The mean value of 6.9 kcal/mole is somewhat higher than the value for a melt with 10% Li_2CO_3.

The value of the viscosity of pure LiCl obtained by extrapolation of the viscosity-composition isotherm at 740°C, obtained in the present work agrees with that reported by Janz [6]. The extrapolation to pure Li_2CO_3 of the viscosity-composition isotherm gives a value for the viscosity of 5.98 centipoises, which is also in good agreement with reported values [6].

All the melts examined have a negative temperature coefficient of surface temperature, $d\gamma/dt$. The temperature coefficients decreased with increasing concentration of Li_2CO_3 except for the composition of 50 mole %. The latter coefficient is higher than the corresponding value for pure LiCl. The temperature coefficients obtained in the present work for two extreme concentrations, 90 mole % LiCl and 30 mole % LiCl, are respectively -0.065 and -0.040 dyne/cm°C. These are close to the respective values of -0.069 and -0.041 dyne/cm°C for pure salts. The change of surface tension with composition shows a point of inflection corresponding to the eutectic composition. The isotherm is slightly convex towards the composition axis. The value of γ for pure LiCl obtained by extrapolation of the γ-composition curve is in good agreement with the value calculated from the equation $\gamma = a - bt$, recommended by Janz [6]. The values reported by Dahl and Duke [11] are lower by 5 dynes cm^{-1} than those obtained in this work. In order to obtain surface tension for pure Li_2CO_3 from the γ-composition plot,

*Cf. reference 6.

a long extrapolation needs to be made. The closest value to pure Li_2CO_3 is that of 70 mole % Li_2CO_3 melt with a surface tension of 189 dynes/cm, that is 55 dynes/cm smaller than the pure compound from the literature [6]. The present extrapolation gives the value of 240 dynes/cm for pure Li_2CO_3. This value compares well with 244 dynes/cm for pure Li_2CO_3 as reported [6].

Part II

SELF-DIFFUSION COEFFICIENTS OF CARBONATE IONS IN $LiCl-Li_2CO_3$ MIXTURE

GENERAL

One of the unknowns in the operation of an oxygen reclamation cell is the mechanism by which CO_2 reaches the electrode. The mechanism may involve the diffusion of either CO_2 in the molecular state or CO_3^{2-} ions which decompose at the electrode surface. An analogous ionic species, such as HCO_3^-, which reflects the presence of a small amount of residual water in the melt, or $LiCO_3^-$ ions with the participation of the cationic constituent, may also be involved in the diffusion. Again, if ionic transport is involved, is the rate-determining step the migration of the carbon-containing species, or is it the reverse, migration of a species such as O^{2-} to the CO_2 adsorption area where CO_3^{2-} or HCO_3^- ions are generated?

In an attempt to gain information on these points, it was decided to measure diffusion coefficients; radioisotope tagging of carbonate ions with C^{14} was used to examine the diffusion of carbonate into a capillary tube from an external phase.

EXPERIMENTAL

Apparatus and Method

The method used was the "into-the-capillary" technique of Bockris and Hooper [19], where diffusion takes place from a radioactive bulk into an inactive capillary.

The diffusion vessel used in this work is the same as that described by Tricklebank, Nanis and Bockris [20] for the determination of diffusion coefficients at high pressure.

Radiochemicals and Preparation of the Radioactive Bath

The radiochemicals were supplied by International Chemical and Nuclear Corp. C^{14} was provided as solid Li_2CO_3 in samples of 5 g each with a specific activity of 10 microcuries per g of Li_2CO_3. Na^{22}, used for checking the apparatus and technique, was provided as solid $NaNO_3$ in samples of 30 g each with a specific activity of 1 microcurie per g of $NaNO_3$. The radiopurity of both radiochemicals was 99%+.

The non-radioactive salts were dried in the same way as is described in Part I of this report. The labelled carbonate was dried at 150°C under CO_2. A sufficient amount of $LiCl-Li_2CO_3$

eutectic mixture* was weighed in a gold-palladium crucible to produce 18 ml of liquid bath containing approximately 50 microcuries of radiotracer. After being melted in a small furnace under CO_2, the mixture was poured into a nickel crucible. The liquid was allowed to solidify and was stored in a dry-box.

Analytical Instruments

The C^{14} (β-emitter) which diffused into capillaries was counted with a PACKARD TRI-CARB liquid scintillation spectrometer Series 314E using standard liquid scintillation procedure. Na^{22} was counted with a 2"×1-3/4" sodium iodide, thallium activated scintillation crystal and photomultiplier tube coupled with a single channel pulse height analyzer, consisting of a Cosmic Radiation Labs Model 1001 "Spectrastat," Model 901 linear amplifier, and Model PA-601 preamplifier.

Capillaries and Filling of the Capillaries

Capillaries of different materials were used. Alumina (99.7%) capillaries 4 cm in length and inner diameter 0.8 mm were sealed at one end in an oxy-coal gas flame. To facilitate sealing, a piece of alumina rod about 2 mm long was inserted to half its length into the tube. The diameter of the rod is such as to fit closely into the tube. The rod melts as soon as the flame touches it, and contracts and welds the tube. Other capillaries used in this work include 90% platinum-10% iridium** (4 cm long, I.D. 1.016 mm), stainless steel 304 (1.100 mm I.D.), and nickel (1.4605 mm I.D.). Diameters of capillaries were determined by a binocular microscope (Carl Zeiss).

Two different cells were used for filling capillaries with the non-active salt. The first was used for filling capillaries with sodium nitrate. This cell is shown in Figure 20. Parts which are placed in the furnace were made of fused silica. The outer tube, A, has an inner diameter of 2.7 cm and length of 44 cm. The inner tube, B, has outer diameter 0.5 cm. Tube B is welded to a cap which joins to the cell by an O-ring. The other end of tube B is welded to a nickel rod to which the capillary holder is threaded. Molten salt is contained in a nickel crucible that can be raised or lowered in much the same way as described in Part I of this report. The procedure for filling capillaries was as follows: Four capillaries are placed on the capillary holder with open ends down. The cap of the cell is then joined with a vacuum line, and the system is evacuated (10^{-2} mm Hg) while the salt is melted. The temperature is set at 20°C below the desired temperature of the run (this procedure insured that the capillaries would be filled at the temperature of the measurement).

* 70:30 mole %

** This alloy rather than platinum is used because of its higher mechanical strength.

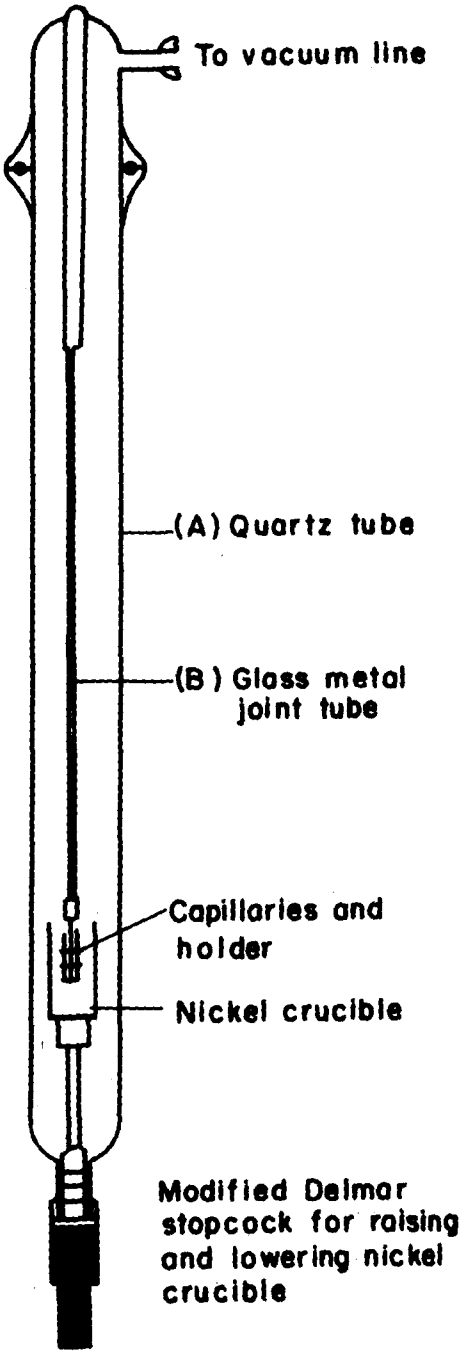

Figure 20. Cell for Filling Capillaries With Molten $NaNO_3$

The capillaries are then immersed into the molten salt by raising the nickel crucible. Release of vacuum with dry nitrogen forced the melt into capillaries. The capillaries, after being withdrawn from the melt and cooled, are placed into a dry-box and stored until use.

Some difficulties were met with in the filling of capillaries with LiCl-Li_2CO_3 melt. Dissolved gas in the melt caused vigorous frothing of the liquid. During the evacuation procedure, the melt was lost from the container and came into contact with the walls of the cell, which were than attacked. A new cell was designed. The base of the cell is made of alumina tube (99.7%) (cf. Fig. 21). The cell is assembled with the aid of a metal flange which is attached to the tube by means of a compression type O-ring seal. For this, the upper part of the alumina tube had to be machined to a true cylinder (52 mm O.D.). Instead of raising the crucible, as was done in the former case, the same mechanism permits the movement of the capillaries. The further procedure for filling capillaries was the same as described above.

Procedure

In order to describe the procedure followed in these experiments, it is necessary to refer to the original scheme of the high temperature and pressure vessel, reproduced in Figures 22 and 23. A stream of CO_2 enters the vessel at C (cf. Fig. 22). A capillary, with the inactive salt in it, is attached to the holder of the vessel in which a container with the active salt is already placed (G, Fig. 23). The apparatus is then assembled with the stirring shaft (K, Fig. 23) in the upper position. The stirring shaft is now lowered by applying pressure in the oil column (K, Fig. 22) so that the opening of the capillary is about 1 cm above the surface of the melt. In this position, the capillary is held for about 5 minutes to reach thermal equilibrium. Then the stirring shaft is lowered to the bottom of its stroke, thus submerging the capillary opening into the melt and initiating the diffusion run. Simultaneously, the V-belt drive is attached to the pulley (N, Fig. 22) and the stirring begun. After the run is completed (3 to 6 hours) stirring is stopped and the capillaries removed from the melt by raising the shaft to its upper position. The radioactive salt is extracted from the capillary, using a stainless steel needle through which a slow flow of water is maintained, and the solution is collected in a beaker. When the salt has been removed, the beaker is placed on a hot-plate to evaporate the solution down to 2 or 3 ml. The solution is then quantitatively transferred into a 25 ml flask. An alumina capillary is placed in a beaker and crushed into small fragments. The salt is then dissolved and the solution is quantitatively transferred to a 25 ml flask.

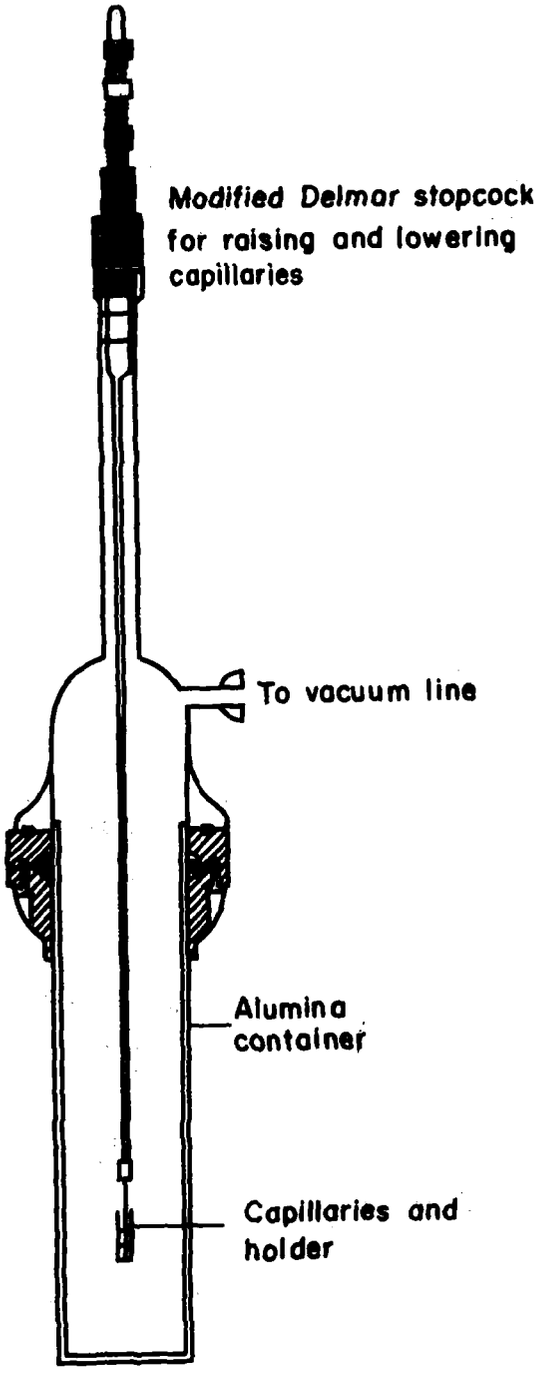

Figure 21. Cell for Filling Capillaries With LiCl - Li_2CO_3 Molten Mixtures

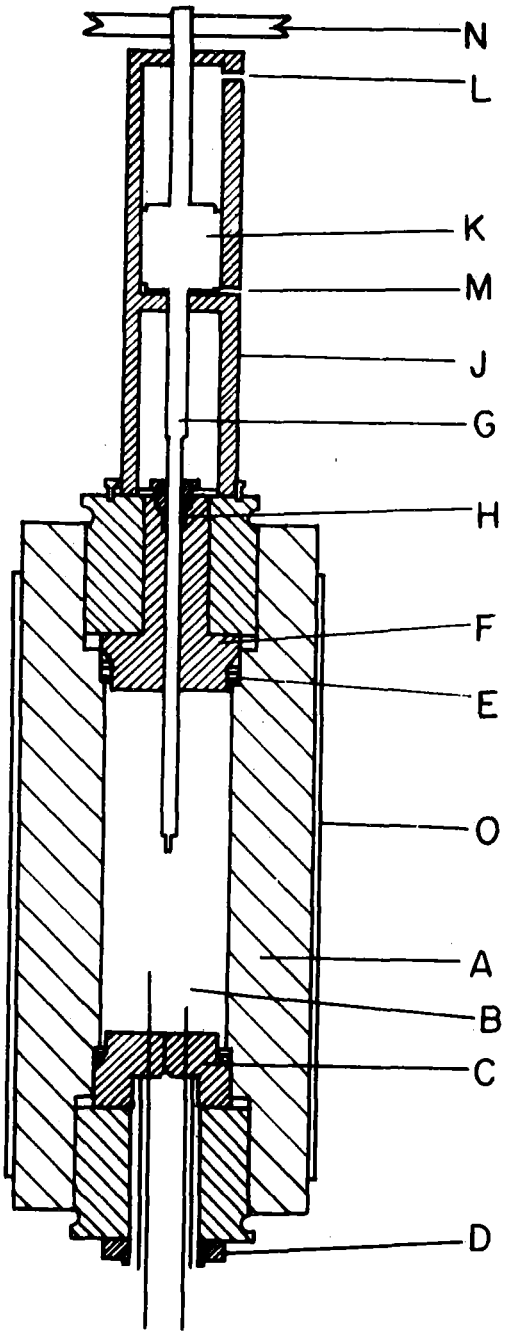

Figure 22. Schematic View of the Pressure Vessel

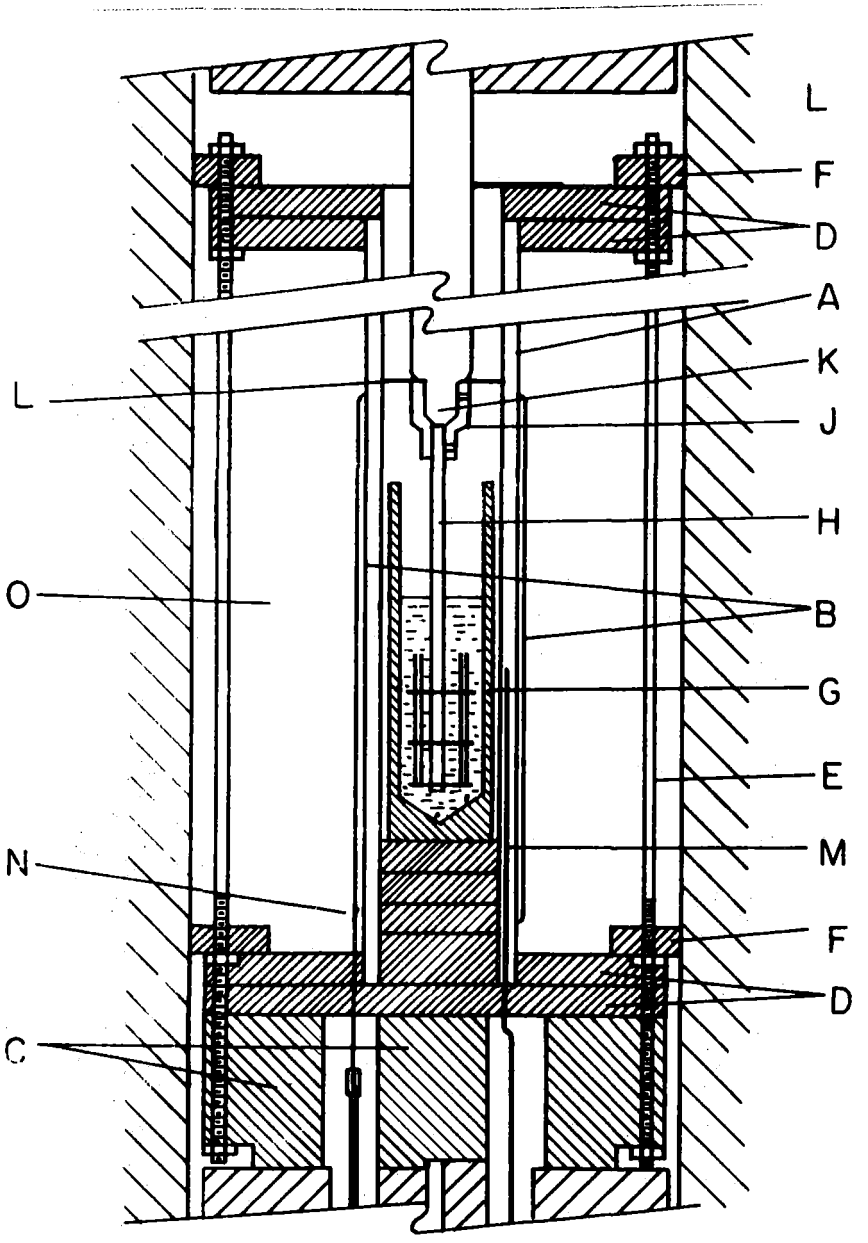

Figure 23. Internal Parts of the Working Chamber

Na^{22} is counted by transferring a 5 ml aliquot of the radioactive solution into the counting tube. For C^{14}, a 12.5 ml aliquot of Bray's [21] scintillator solution is admitted to the counting bottle together with 2 ml of the aliquot of the radioactive solution.

The diffusion coefficient, D, is given by the equation [20, 22]:

$$Q = C_0 \frac{\pi d^2}{2} \left(\frac{Dt}{\pi}\right)^{\frac{1}{2}}$$

where d is diameter of the capillary, Q the total amount of diffusate in the capillary at time t, and C_0 is the specific activity of the bath sample and is calculated from the following expression:

$$C_0 \text{ (cpm cm}^{-3}) = K \frac{\rho}{W}$$

where K is total activity (counts per minute) from a bath sample of mass W(g) and ρ is the density of the molten salt at the temperature of the experiment. In order to maintain boundary conditions for the application of the former equation, a minimum rate of flow past the opening of the capillary is required to keep the concentration at the opening of the capillary equal to that of the bulk. It has been established [22] that the rotation of the capillary causes a cylindrical "slug" of inactive salt to be swept out of the capillary and replaced by radioactive salt from the bath. This slug, of length $\Delta\ell$, adds to the measured Q a value equal to $C_0(\pi d^2/4)\Delta\ell$. A correction to Q for this value is made. The length of $\Delta\ell$ is obtained from the plot of $\Delta\ell/d$ vs. Reynolds number [23]. The Reynolds number is defined as

$$N_{Re} = \frac{vd}{\nu} = \frac{2\pi Rw\rho d}{60\eta}$$

where R is the radius of rotation (cm), ρ the density (g cm^{-3}), η the viscosity (g cm^{-1} sec^{-1}), ν the kinematic viscosity (cm^2 sec^{-1}), w the rotation rate (rpm), and v is the linear velocity of the capillary mouth (cm sec^{-1}). Thus, with this correction, D is calculated from the equation

$$Q - C_0 \frac{\pi d^2}{4} \Delta\ell = C_0 \frac{\pi d^2}{2} \left(\frac{Dt}{\pi}\right)^{\frac{1}{2}}$$

RESULTS

As a check on the apparatus and technique, the self-diffusion coefficient of Na^{22} in $NaNO_3$ was measured and compared with the values of Tricklebank, Nanis and Bockris [22], who report the diffusion coefficient at 350°C and 1 bar as $(2.10\pm0.09)\times10^{-5}$ cm^2 sec^{-1}. In this work a value of $(2.08\pm0.10)\times10^{-5}$ cm^2 sec^{-1} was obtained.

The activity of C^{14} in the liquid bath was found to decrease with time (exchange with CO_2 atmosphere). The loss was about 26% at 560°C after an experiment of five hours. The diffusion coefficients were calculated taking the arithmetic mean of the number of counts of the liquid bath, before and after the experiment.

The values of self-diffusion coefficients for carbonate ions in $LiCl-Li_2CO_3$ eutectic mixture are given in Table 37. The dependence of the diffusion coefficients on temperature is shown in Figure 24. The activation energy calculated therefrom is 10.0±1.5 kcal/mole. It is interesting to note that for the diffusion of $CO_3^{=}$ ions in pure carbonates or in mixtures of carbonates, the diffusion coefficient was found to be also close to 10 kcal/mole.

Self-Diffusion Coefficient

The maximum error in the measurements of self-diffusion by diffusion into the capillary technique was established by Bockris, Yoshikawa and Richards [24]. They found that the maximum error is given by:

$$\frac{\delta D}{D} = \frac{\delta t}{t} + 2\left\{\frac{\delta \frac{4Q}{\pi d^2 C_0} + \delta\Delta\ell}{\frac{4Q}{\pi d^2 C_0} - \Delta\ell}\right\}$$

with

$$\delta\left(\frac{4Q}{\pi d^2 C_0}\right) = \frac{4}{\pi}\left[\frac{\delta Q}{d^2 C_0} + \frac{2Q\delta d}{d^3 C_0} + \frac{Q\delta C_0}{d^2 C_0^2}\right] \quad .$$

The substitution of the appropriate maximum probable errors in each of the measured quantities gives a value of 15% for $\delta D/D \times 100$. This is the error in each capillary. Since two to four capillaries were used in each experiment, the maximum error in the mean value is about 9%. In the present work, this error was even further reduced. The accuracy in counting C_0 and Q has been increased considerably by using a liquid scintillation spectrometer with greater counting efficiency than the gas flow proportional counting system used in the early work. The duration of experiments was of the order of 3 to 6 hours in the present work; in the early work the experiments were of the order of 2 hours. As has been mentioned before, the activity of C^{14} in the liquid bath has been found to decrease with time, and the change at 560°C was found to be 26% after an experiment of 5 hours. The diffusion coefficients were calculated taking the arithmetic mean of the number of counts of the liquid bath, before and after the experiments. This introduces an uncertainty of about 7% in the values reported.

TABLE 37. DIFFUSION OF $C^{14}O_3^{=}$ IONS IN MOLTEN $LiCl-Li_2CO_3$ EUTECTIC MIXTURE (70:30 Mole%)

Capillary	Temperature (°K)	Diffusion Coefficient $D \times 10^5$ ($cm^2\ sec^{-1}$)
Nickel	803	1.15
"	"	0.94
"	"	1.04
"	"	0.96
"	833	1.20
"	"	1.45
"	"	1.16
"	876	1.89
"	"	1.86
"	898	1.92
"	"	1.98
"	918	2.14
"	"	2.45

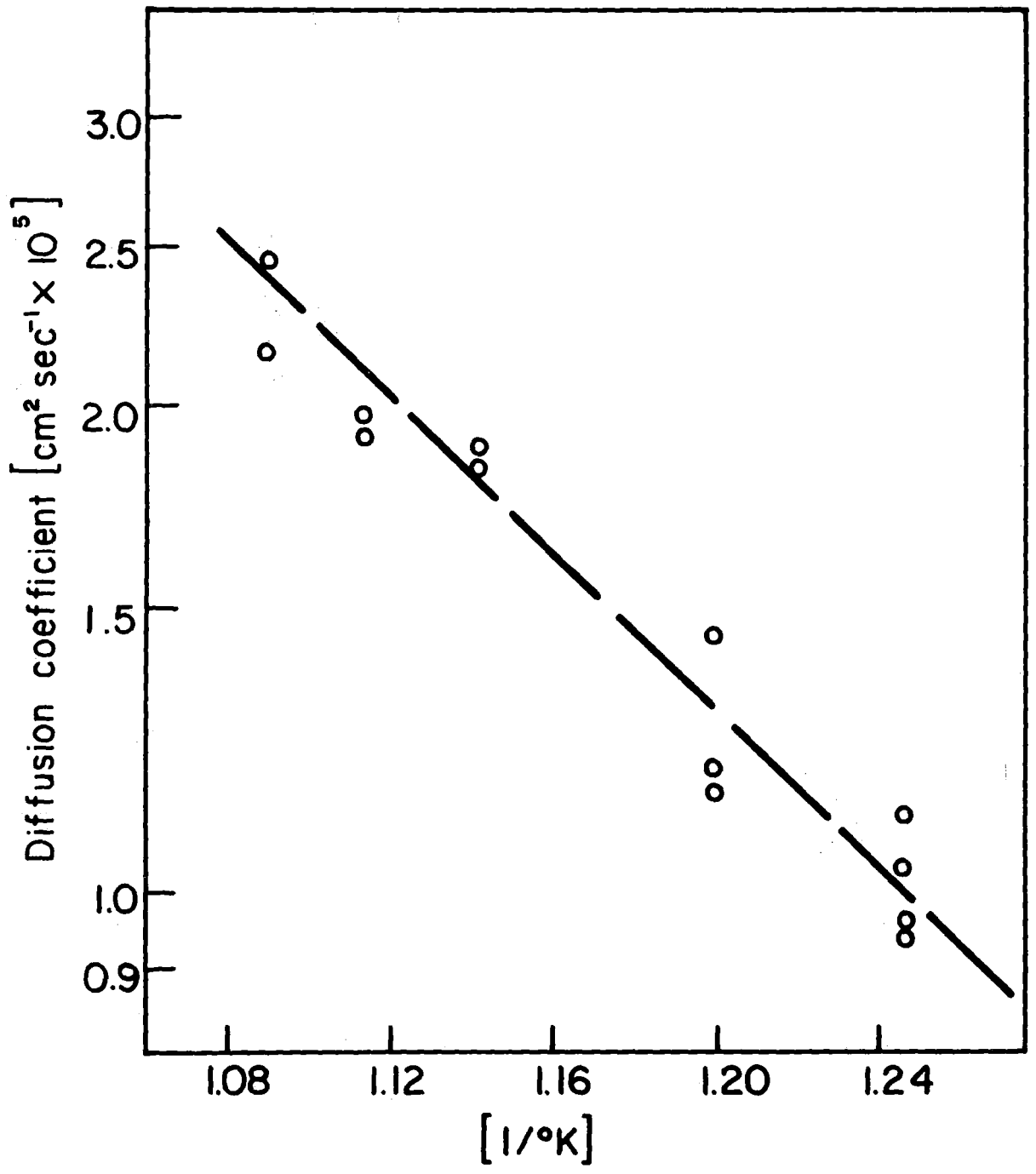

Figure 24. Diffusion Coefficient of $C^{14}O_3^=$ in LiCl - Li_2CO_3 Eutectic Mixture

REFERENCES

1. M.S. White and C. Solomons, Annual Report for 1966-67, AEC Contract No. AT30-1-1769, Section 2 (14 July 1967).

2. C. Solomons and M.S. White, Annual Report for 1966-67, AEC Contract No. AT30-1-1769, Section 3 (14 July 1967).

3. M.S. White and C. Solomons, Linear Oscillation Viscometer, submitted to Rev. Sci. Instr.

4. C. Solomons and M.S. White, Oscillating-Plate Viscometry, Part I, Theoretical Principles, for submission.

5. J. Timmerman, *Physicochemical Constants of Pure Organic Compounds* (Elsevier Publishing Company, Inc., New York and Amsterdam, 1950).

6. G.J. Janz, *Molten Salt Handbook* (Academic Press, New York, 1967).

7. "Mechanical Properties of Metals and Alloys," National Bureau of Standards, Circular C-447.

8. G.J. Janz and M.R. Lorenz, Rev. Sci. Instr., *31*, 18 (1960).

9. H. Bloom, I.W. Knaggs, J.J. Molloy and D. Weleh, Trans. Faraday Soc., *49*, 1458 (1953).

10. G. Bertozzi and G. Sternheim, J. Phys. Chem., *68*, 2908 (1964).

11. J.L. Dahl and F.R. Duke, AEC Report Contract No. 7405-Eng-82 (June 1957).

12. W. Rafalski and C. Solomons, Controlled Atmosphere Sessile Drop Cells, submitted to Rev. Sci. Instr.

13. C. Solomons, Telemacroscopic Camera for Moderate Magnifications at Long Working Distances, in preparation for Rev. Sci. Instr.

14. H.A. Laitinen and J.W. Pankey, J. Am. Chem. Soc., *81*, 1053 (1959).

15. F. Bashforth and J.C. Adams, An Attempt to Test the Theories of Capillary Action (Cambridge University Press, 1883).

16. A.W. Porter, Phil. Mag., *15*, 163 (1933).

17. G.J. Janz and F. Saegusa, J. Electrochem. Soc., *110*, 452 (1963).

18. G.J. Janz and M.R. Lorenz, J. Electrochem. Soc., *108*, 1052 (1961).

19. J.O'M. Bockris and G.W. Hooper, Discussions Faraday Soc., *32*, 218 (1962).

20. S.B. Tricklebank, L. Nanis and J.O'M. Bockris, Rev. Sci. Instr., *35*, 807 (1964).

21. G.A. Bray, Anal. Biochem., *1*, 279 (1960).

22. S.B. Tricklebank, L. Nanis, and J.O'M. Bockris, J. Phys. Chem., *68*, 58 (1964).

23. S.R . Richards, Ph.D. Thesis, University of Pennsylvania (1964).

24. J.O'M. Bockris, S. Yoshikawa and S.R. Richards, J. Phys. Chem., *68*, 1838 (1964).

POSSIBLE DIRECTIONS FOR FUTURE WORK

There are still needs for more experiments and data of technological importance. In particular:

1. Systematic extension should be made of the measurements of surface tension, viscosity, and contact angle to a series of sodium carbonate-lithium oxide melts of various compositions. There should be about 10 to 15 compositions so that a proper analysis of the data could be made.

2. With each of these measurements, there should be a variation of temperature, so that the appropriate heats of activation could be obtained.

3. There should be a considerable extension of the as-yet-abortive experiments on the detection of $O^{=}$ and other radicals present in the solution by means of transient analysis. There are many opportunities here, and considerable progress could be made. However, it would not perhaps be a matter of simple potentiostatic and/or galvanostatic analysis, as the transients are very brief and AC polarography might have to be used in the initial stages.

4. Diffusion work: The main object of the diffusion work is as an aid to the detection of radicals present. It would be helpful to work with C^{14}, Na^{24}, and O^{18}, as markers in diffusion measurements. This would enable us to distinguish between radicals present.

5. The Department of Chemistry at the University of Pennsylvania has good Raman equipment for doing Raman spectra of molten salts. This has been used extensively in the Department for investigation of complexes appearing in molten salts. This, too, would be a likely method for investigating possible complexes existing in carbonate systems. It would also elucidate the existence of radicals relevant to diffusion.